

Fault-tolerant syndrome extraction in $[[n, 1, 3]]$ non-CSS code family generated using measurements on graph states

Harsh Gupta,* Mainak Bhattacharyya,† Ritik Jain,‡ and Ankur Raina§

Department of Electrical Engineering and Computer Science,
Indian Institute of Science Education and Research Bhopal, 462066 Bhopal, India

(Dated: November 11, 2025)

The reliability of quantum computation critically depends on the performance of quantum error-correcting codes (QECCs), which can be severely degraded by hook errors that reduce the effective code distance. In this work, we construct a family of $[[n, 1, 3]]$ non-CSS QECCs to achieve fault-tolerant (FT) syndrome measurement, where $6 \leq n \leq 10$. We employ the bare-ancilla method of Muyuan Li *et al.* to demonstrate fault tolerance in the presence of hook errors during syndrome extraction. We present a systematic protocol for generating these QECCs using graph codes. Using a custom lookup-table decoder, we simulate the code's performance under both anisotropic and circuit-level depolarizing noise. Our results reveal a trade-off in performance with respect to the code rate and identify optimized codes under these noise models. We benchmark our results against the infamous flag-qubit method of Chao *et al.*. Notably, we introduce a code with improved code rate while maintaining the same distance as the work of Muyuan Li *et al.* Our approach facilitates the identification and construction of a family of distance three FT non-CSS QECCs.

Keywords: Fault Tolerance, Non-CSS Quantum codes, Hook Errors, Bare Ancilla, Flag error correction.

I. INTRODUCTION

Quantum devices continue to evolve, though their increased susceptibility to environmental noise remains a major obstacle to scalability. In quantum computation, operations on qubits must be executed with high fidelity to suppress errors in the final outcomes. As a result, the development of a robust Quantum Error Correcting Code (QECC) is fundamental to achieving fault-tolerant (FT) quantum computing. Implementing QECCs in practical scenarios presents significant challenges, with fault tolerance being a major requirement. During a computation, fault tolerance can be achieved if the error rate is below a certain threshold [1, 2]. Crucially, the process of syndrome extraction must also be implemented in an FT manner to prevent the propagation of errors into the data qubits. One of the earliest codes tested for fault tolerance on small systems is the $[[4, 2, 2]]$ QECC using ion trap and superconducting qubits [3, 4]. They demonstrated that error detection can improve certain simple sampling tasks. This code only detects a Pauli error as its minimum distance is two. Any limited error-correcting capacity of a QECC imposes significant resource overhead required for FT quantum computation. Several techniques have been proposed for FT syndrome extraction. Steane's method requires an FT logical state in the syndrome measurement, whereas Shor's method requires extra qubits prepared in the cat state for FT syndrome measurement [5, 6]. Similarly, Knill's method uses a logical Bell pair [7].

Researchers have shown that stabilizers outside the minimal generating set can be leveraged to strengthen the error-correcting capability of quantum codes [8]. Fujiwara proved that it is possible to detect the measurement error of the syndrome qubit even in $[[5, 1, 3]]$ QECC [9]. Yoder *et al.* address that both $[[5, 1, 3]]$ and $[[7, 1, 3]]$ QECCs can be made resistant to hook errors using three and two additional qubits, respectively [10]. Using extra two qubits, Chao and Reichardt were able to correct the faults of distance-three codes that lead to correlated errors in data qubits during syndrome extraction [11]. Muyuan Li *et al.* proposed the bare method, a FT syndrome extraction scheme on a $[[7, 1, 3]]$ QECC using only one ancillary qubit by cleverly reordering the operators of stabilizers. This method ensures no logical error occurs in data qubits due to a single Pauli error on the ancillary qubit [12]. The authors in [12] find the logical error rate for anisotropic noise below the pseudo-threshold limit. The procedure by which this specific $[[7, 1, 3]]$ code is identified is not explicitly described. This observation motivates the search for the family of $[[n, 1, 3]]$ QECCs of this type. In addition, we explore the existence of QECCs with improved code rate that similarly prevent the occurrence of hook errors due to a single Pauli error on the ancillary qubit.

In this paper, we introduce a new family of $[[n, 1, 3]]$ QECCs, *bare ancilla codes* (BACs), which enable FT syndrome extraction without requiring extra verification or flag qubits [11]. BACs exploit the structure of graph codes with a parity check matrix to achieve fault tolerance with only a bare ancilla qubit [13–16]. A custom lookup-table decoder is constructed, where hook errors are corrected by reordering the arrangement of operators in a stabilizer within the syndrome extraction circuit. We analyze the codes' performance under both anisotropic and depolarizing noise models and benchmark it against the flag-qubit method. Our results show that BACs pro-

* harsh22@iiserb.ac.in

† mainak23@iiserb.ac.in

‡ ritikjain@iiserb.ac.in

§ corresponding author: ankur@iiserb.ac.in

vide FT quantum error correction with better or competitive performance in most cases considered in this paper. The structure of the paper is as follows. In Sec. II, we discuss the Calderbank-Shor-Steane (CSS) and non-CSS QECCs, along with the review of techniques used to make QECCs FT during syndrome measurement. Graph code construction using parity check matrix is given in the Sec. III, which will be used for BAC construction. In Sec. IV, we present an algorithm to construct a BAC given a non-CSS stabilizer. Experimental setup with noise models is discussed in Sec. V. Simulation results, which include logical and total error rates are reported in Sec. VI. We conclude the paper in Sec. VII.

II. BACKGROUND AND PRELIMINARIES

QECCs form the foundation for protecting quantum information against decoherence and operational errors. We shall briefly discuss some basic concepts necessary to understand the rest of the paper in this section.

A. CSS and non-CSS codes

In 1995, Shor introduced the first scheme capable of correcting arbitrary single-qubit errors using nine physical qubits, that is, at a code rate of 1/9 [17]. Steane subsequently introduced a seven-qubit code with a higher code rate of 1/7 [18]. Laflamme *et al.* later established the five-qubit “perfect” code, which saturates the quantum hamming bound and achieves the minimum block size required to protect a single logical qubit from any single-qubit error [19]. While these codes differ in code length, they share the same minimum distance and therefore show the equivalent error-correction capability. This line of work can be unified under the stabilizer formalism, where an $[[n, k, d]]$ stabilizer code is defined as the joint $+1$ eigenspace of an Abelian subgroup \mathcal{S} of the Pauli group P_n on the Hilbert space $(\mathbb{C}^2)^{\otimes n}$ [20]. A key subclass is formed by Calderbank-Shor-Steane (CSS) codes, which are constructed from two classical linear codes with parity-check matrices \mathbf{H}_x and \mathbf{H}_z such that $C_Z^\perp \subseteq C_X$ and $C_X^\perp \subseteq C_Z$ [21]. CSS codes address bit-flip and phase-flip errors independently, while non-CSS codes handle both simultaneously [19]. In addition, non-CSS codes are not restricted by the structural constraints that govern CSS code design and have the potential to exceed the performance limits of CSS schemes and approach the hashing bound of a quantum channel [22]. Algebraically for a stabilizer code with parity check matrix $\mathbf{H} = [\mathbf{H}_x | \mathbf{H}_z]$, the following relation holds

$$\mathbf{H}_z \mathbf{H}_x^T + \mathbf{H}_x \mathbf{H}_z^T = \mathbf{0}. \quad (1)$$

Achieving fault tolerance in these QECCs also requires error-free syndrome extraction using ancilla qubits. An error in ancilla can spread to data qubits through two-qubit gates, leading to so-called hook errors.

B. Hook Errors in QEC

Syndrome measurements in quantum error correction are typically performed by coupling ancilla qubits to several data qubits through two-qubit controlled gates such as CNOT or CZ gates [2]. Pauli errors that occur on the ancilla qubit can propagate through these interactions and generate correlated errors on the data qubits. They are called hook errors, since a single ancilla fault can effectively hook onto multiple qubits instead of remaining confined to one [23]. Hence, a single physical fault in a syndrome qubit propagates to the data qubit and converts into two or more qubit errors. Therefore, meticulous circuit design is important to evade hook errors. If left untreated, hook errors reduce the effective code distance and can significantly limit the error correcting capability of the code.

C. Related works

Over the past decade, major advances have been made in developing fault-tolerant syndrome measurement schemes. Fujiwara identified a previously unrecognized property of stabilizers in quantum error-correcting codes [9]. He demonstrated that using combinations of stabilizers outside the minimal generating set, traditionally considered redundant, can enhance error-correcting capability. Building on this idea, Ashikhmin *et al.* generalized existence theorems and extended the quantum singleton bound to incorporate measurement redundancy [24]. Crow *et al.* showed that redundant stabilizers can result in error thresholds comparable to those of conventional measurement-based methods without explicit measurement, often called measurement-free quantum error correction [25]. Subsequently, various approaches have been proposed to exploit redundancy in syndrome extraction, though these techniques primarily address errors in syndrome qubit measurements [26, 27]. Yoder and Kim demonstrated that hook errors arising from interactions between syndrome qubits and data qubits can also be corrected via a suitably designed framework, requiring significant overhead [10]. Chao and Reichardt later addressed this issue by introducing a more resource-efficient scheme that requires only two additional qubits, an ancilla qubit and a flag qubit [11]. This approach is applicable to all stabilizer codes [28, 29]. Subsequent work produced several variants of the flag-qubit method, optimizing circuit depth through dynamic and adaptive selection of stabilizer measurements and introducing tools to simulate and optimize the flag approach [30–34]. Lao and Almudever extended this approach by introducing a geometrical interaction mapping [35]. They combine flag fault tolerance with quantum circuit mapping to create an efficient flag-bridge implementation of FT quantum error correction on near-term devices.

Muyuan Li *et al.* introduced a $[[7, 1, 3]]$ non-CSS stabilizer code that uses clever reordering of stabilizers with only one ancilla qubit while measuring the syn-

drome [12]. They analyzed the code performance under anisotropic and depolarizing noise and revealed that the code performs best in the anisotropic regime, a noise commonly encountered in trapped ion systems [36]. Researchers used a similar reordering method with a bare ancilla qubit for constructing the FT syndrome measurement circuit for Bacon-Shor code and compass codes [37, 38]. Maheshwari *et al.* analyzed a $[[8, 1, 3]]$ non-CSS QECC, reporting its pseudo-threshold under both depolarizing and anisotropic noise models using a bare ancilla qubit [39]. Despite these advances in the bare ancilla method, which reduce resource cost, their performance degrades under depolarizing noise or is constrained by hardware-specific assumptions, for example, in trapped-ion implementations [23]. Moreover, a systematic framework for constructing non-CSS stabilizer codes that mitigate hook errors while maintaining a higher code rate has yet to be developed. Motivated by this gap, we construct a family of $[[n, 1, 3]]$ codes inspired by graph codes using a bare ancilla qubit for syndrome extraction. The following section introduces graph codes, which serve as the foundation for our code construction.

III. NON-CSS FAMILY OF QUANTUM CODE CONSTRUCTIONS USING MEASUREMENTS

We now discuss how the message qubit information is encoded using measurements. Stabilizer evolution under measurement is described using some of the methods adapted from the Measurement-based-quantum-computing (MBQC) setting.

A. MBQC method

MBQC was introduced by Raussendorf *et al.*, which differs from the network-based quantum computing models due to the measurement-based operations [40]. Within this framework, quantum computation is carried out by first preparing and then entangling qubits into a highly structured resource state. This so-called cluster or graph state is represented by an undirected graph $G = (V, E)$, shown in Figure 1, where V denotes the set of vertices corresponding to the qubits, and E represents the edges corresponding to the CZ gates between the qubits.

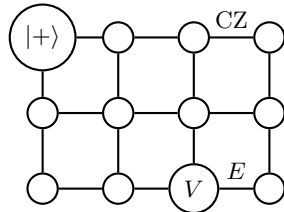


FIG. 1. A Cluster state, which is also depicted as an undirected graph $G = (V, E)$ where V is the set of vertices corresponding to qubits, each initialized with $|+\rangle$ state and E is the set of edges, each corresponding to a CZ gate.

In order to move from the description of graph states to the construction of QECCs, it is important to recall how the measurement outcomes affect the stabilizer structure of a graph state. The evolution of stabilizers under specific measurement choices provides the foundation for relating cluster states to error-correcting codes. A formal derivation of the stabilizer generators of post-measurement states can be found in [2], while the detailed behavior of stabilizer sub-groups under various measurement settings is described in [41, 42]. This perspective naturally motivates the construction of quantum error-correcting codes from graph states, commonly referred to as graph codes. The concept of graph codes was first introduced by Schlingemann and Werner, where the code space is defined through an isometry from input qubits to output qubits using a graph and a finite Abelian group [13, 43]. Further, Schlingemann and Grassl *et. al* independently showed that every stabilizer QECC can be represented as graph code and vice versa [44, 45]. Graph codes defined in [13, 43] are also constructed using measurements on the message qubit. When k message qubits are combined with n qubits of the graph through CZ gates, we call it an $(n+k)$ qubit graph-message state. Then encoding can be implemented by measuring the message qubits in the X basis, as shown in Figure 2 [46].

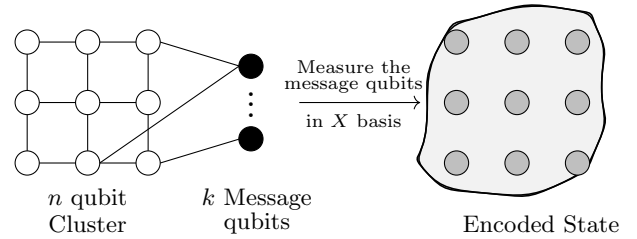


FIG. 2. The message qubits (●) are encoded into the cluster by measuring it in the X basis.

Each stabilizer of the $(n+k)$ qubit graph-message state is given by Eq. (2):

$$g_j = X_j \prod_{i \in \mathcal{N}_j} Z_i, \quad j \in \{1, 2, \dots, n\}, \quad (2)$$

where \mathcal{N}_j denotes the neighbours of the j^{th} cluster qubit. The parity check matrix corresponding to Eq. (2) can be written in an elegant form as [47]:

$$\mathbf{H} = [\mathbf{H}_x \mid \mathbf{H}_z] = [\mathbf{I}_{n \times n} : \mathbf{0}_{n \times k} \mid \mathbf{A}_{n \times n}^{cc} : \mathbf{A}_{n \times k}^{cm}], \quad (3)$$

where $\mathbf{A}_{n \times n}^{cc}$ is an adjacency matrix associated with the cluster state of $(n+k)$ graph-message state. $\mathbf{A}_{n \times k}^{cm}$ matrix indicates the connection of the message qubits to the cluster qubits. $\mathbf{I}_{n \times n}$ is the identity matrix and $\mathbf{0}_{n \times k}$ is the NULL matrix.

In this work, we use the same encoding procedure as shown in Figure 2, adopted from [46], whose formal proof is provided in Appendix A. The encoded state is

obtained by transformations to the parity-check matrix of the $(n+k)$ qubit graph-message state.

B. Encoding of message qubits

Let the generators of stabilizer group of $(n+k)$ qubit graph-message state be

$$\langle g_1, g_2, \dots, g_{n-k} \rangle.$$

To encode a message on the $(n+i)^{\text{th}}$ qubit, the stabilizer set is modified following the procedure in [41]. Algorithm-1 is the pseudo-code representation of these steps using a parity check matrix. At each iteration, a pivot row with a ‘1’ in the $(n+i)^{\text{th}}$ column of \mathbf{H}_z of message qubit is selected, and the pivot is added (modulo 2) to all other rows containing a ‘1’ in that column, thereby isolating the qubit in a single stabilizer. The pivot row and the two columns corresponding to the measured qubit are subsequently removed. Repeating this procedure for all k message qubits reduces the matrix dimension from $n \times 2(n+k)$ to $(n-k) \times 2n$, resulting in the stabilizer description of the encoded, generally non-CSS, $[[n, k, d]]$ code in the MBQC framework.

Algorithm 1: Graph code stabilizer construction via parity check matrix using measurements

Input: Parity-check matrix
 $\mathbf{H} = [\mathbf{H}_x \mid \mathbf{H}_z] = [\mathbf{I}_{n \times n} : \mathbf{0}_{n \times k} \mid \mathbf{A}_{n \times n}^{\text{cc}} : \mathbf{A}_{n \times k}^{\text{cm}}]$
Output: Updated matrix \mathbf{H} of dimension
 $(n-k) \times 2n$

```

1  $m \leftarrow k$ 
2 for  $\text{iter} \leftarrow 1$  to  $k$  do
3    $\text{target} \leftarrow 2(n+m)$ ,  $\text{pivot} \leftarrow \emptyset$ 
4   for  $i \leftarrow 1$  to  $\text{row}(\mathbf{H})$  do
5     if  $\mathbf{H}[i][\text{target}] = 1$  then
6        $\text{pivot} \leftarrow i$ 
7       break
8   for  $j \leftarrow 1$  to  $\text{row}(\mathbf{H})$  do
9     if  $j \neq \text{pivot}$  and  $\mathbf{H}[j][\text{target}] = 1$  then
10       $\mathbf{H}[j] \leftarrow \mathbf{H}[j] + \mathbf{H}[\text{pivot}] \bmod 2$ 
11    $\mathbf{H} \leftarrow \mathbf{H}[:, \{1, \dots, 2(n+k)\} \setminus \{n+m, \text{target}\}]$ 
12    $\mathbf{H} \leftarrow \mathbf{H}[\{1, \dots, n\} \setminus \{\text{pivot}\}[:, :]$ 
13    $m \leftarrow m - 1$ 
14 return  $\mathbf{H}$ 

```

1. Finding logical operators

Any $[[n, 1]]$ QECC is associated with two logical operators, X_l and Z_l , that (i) commute with all stabilizer generators and (ii) anti-commute with each other. In QECCs derived from the MBQC framework, these logical operators can be identified directly from the pre-measurement parity-check matrix. The logical Z_l operator corresponding to the i^{th} message qubit is obtained from the $(n+i)^{\text{th}}$ column of the \mathbf{H}_z block: every entry 1 in this column indicates a Pauli-Z acting on the

corresponding physical qubit. The logical X_l operator is determined from the pivot row of the parity-check matrix, restricted to the first n qubits. Finally, to achieve code distance d , the message node must be connected to at least d qubits, i.e., it must have degree $\geq d$ (Appendix- A).

Overall, this matrix-based formulation offers a systematic way to encode message qubits and track stabilizer updates under measurement, while at the same time providing a direct route to extract logical operators and distance conditions from the graph structure. This avoids circuit-level constructions and enables a more transparent analysis of non-CSS codes within the MBQC framework.

IV. BARE ANCILLA CODE CONSTRUCTION

For each stabilizer g , we permute the order of gates used in syndrome extraction to obtain distinct syndromes. Our approach explores which permutation in the measurement strategy leads to distinct syndromes for hook errors generated due to errors on the ancilla qubit. Therefore, we would like to construct such stabilizers that facilitates FT syndrome extraction using the permutation trick.

We observe that non-CSS FT QECCs, discussed in [12] and [39], can be generated using measurements on the corresponding graph states as discussed in Sec. III. We introduce a protocol that gives rise to a family of $[[n, 1, 3]]$ FT non-CSS QECCs derived from graph codes. Further, we establish the conditions under which this family remains FT against hook errors and provide bounds on their error-correcting capabilities.

A. Algorithm to find the BACs

We first define a modified parity-check matrix to find the syndrome corresponding to a single-qubit error as:

$$\mathbf{H}_{\text{xyz}} = [\mathbf{H}_x \mid \mathbf{H}_z \mid \mathbf{H}_x \oplus \mathbf{H}_z]. \quad (4)$$

For each stabilizer generator g of weight $w_g > 2$, Algorithm 2 systematically enumerates all admissible permutations of the Pauli operators that constitute g . To elaborate on this idea, we consider a stabilizer generator

$$g = \prod_{a_i=1}^{w_g} P_{a_i}$$

where $P \in \{X, Y, Z\}$ and $(a_1, a_2, \dots, a_{w_g})$ indicates the order of ancilla-controlled Pauli gates acting on the data qubits. Treating each of the subsequences of Pauli operators as potential hook errors, we check the syndromes corresponding to these errors, occurring due to single-qubit Pauli errors in the ancilla qubit. The Algorithm 2 exhaustively enumerates the syndromes for all errors, namely single-qubit errors and hook errors. If any permutation gives a zero syndrome or a duplicate syndrome, it is discarded, ensuring that only unique nontrivial mappings are retained.

The valid mappings are recorded in two structures:

(a) μ_o contains subsequences of the stabilizer g and its corresponding syndromes, and (b) μ_a contains variants of each subsequence where every variant is obtained by substituting the last element in the subsequence by all Pauli operators X, Y, Z together with their syndromes. The overall worst-case runtime is $\mathcal{O}(w_g!w_g)$, but backtracking with early pruning and symmetry reduction reduces the effective search space in practice.

Algorithm 2: Permutation-based construction of stabilizer syndromes

Input: $\mathbf{H}_{xyz} = [\mathbf{H}_x | \mathbf{H}_z | \mathbf{H}_x \oplus \mathbf{H}_z]$,
 Stabilizer $g = \prod_{a_i=1}^{w_g} P_{a_i}$, $P \in \{X, Y, Z\}$ with
 $w_g > 2$
Output: μ_o, μ_a lists.

- 1 Initialize $\mu_o, \mu_a \leftarrow \emptyset$
- 2 $\text{syn}(P_{a_1})$: syndrome of P_{a_1}
- 3 **foreach** permutation π of g **do**
- 4 $\tilde{g} \leftarrow [P_{\pi(1)}, \dots, P_{\pi(w_g)}]$; $\nu_o, \nu_a \leftarrow \emptyset$
- 5 **for** $i \leftarrow 2$ **to** $w_g - 1$ **do**
- 6 **foreach** $M \in \{X, Y, Z\}$ **do**
- 7 **if** $(w_g = 3)$ **or** $(i = w_g - 1)$ **then**
- 8 **if** $M_i = P_{\pi(i)}$ **then**
- 9 **continue**
- 10 $\delta \leftarrow (\text{syn}(M_i) + \text{syn}(P_{\pi(i-1)})) \bmod 2$
- 11 **if** $\delta = 0$ **or** $\delta \in \nu_a$ **then**
- 12 **discard** \tilde{g} ; **break**
- 13 $\nu_a \leftarrow ([P_{\pi(1)}, \dots, P_{\pi(i-1)}, M_i], \delta)$
- 14 **if** $M_i = P_{\pi(i)}$ **then**
- 15 $\nu_o \leftarrow ([P_{\pi(1)}, \dots, P_{\pi(i)}], \delta)$
- 16 $\text{syn}(P_{\pi(i-1)}) \leftarrow \text{syn}(P_{\pi(i-1)}) + \text{syn}(P_{\pi(i)})$
 $\quad \quad \quad \text{mod 2 addition}$
- 17
- 18 $\mu_o, \mu_a \leftarrow \nu_o, \nu_a$
- 19 **return** μ_o, μ_a

B. Fault Tolerance of BACs

The FT nature of the BACs depends on the weight of the stabilizers. The key to deriving the conditions of correctable errors for the BAC depends on the availability of unique syndromes. For instance, the number of distinct non-zero syndromes for any possible single data qubit Pauli error for a given \mathbf{H}_{xyz} is defined as follows

$$\kappa(\mathbf{H}_{xyz}) := |\{s(E) \neq 0 : E \in \{X_i, Y_i, Z_i\}, i \in \{1, \dots, n\}\}|,$$

where $s(E)$ refers to the syndrome for error E . Since the total cardinality of the non-zero syndromes for $[[n, k, d]]$ stabilizer codes is $2^{n-k} - 1$, the number of nonzero syndrome patterns unused after assignment of syndromes to single-qubit Pauli errors on the data qubit is

$$S_u = 2^{n-k} - 1 - \kappa(\mathbf{H}_{xyz}). \quad (5)$$

For syndrome measurement of $[[n, 1, 3]]$ QECCs, consider a stabilizer generator $g = \prod_i P_{a_i} \in \mathcal{S}$. $\rho_g(a_i)$ represents the hook error propagating into the data qubits when an error occurs on the ancilla qubit before the two-qubit controlled-Pauli gate, namely $C-P_{a_i}$. Therefore, we consider the occurrence of errors in the ancilla qubit at w_g locations, also indexed using a_1, a_2, \dots, a_{w_g} respectively as indicated in Figure 3. \mathcal{U}_g is a set of uncorrectable hook errors for a given stabilizer g , defined as

$$\mathcal{U}_g = \{\rho_g(a) : w(\rho_g(a)) > 1, w(\rho_g(a)s) > 1 \forall s \in \mathcal{S}\},$$

where $w(E)$ denotes the weight of the error E . Suppose $g = P_3 P_4 P_1 P_2 P_5$, then the order of controlled-Pauli gates $(a_1, a_2, a_3, a_4, a_5)$ is equal to $(3, 4, 1, 2, 5)$. Hook error $\rho_g(a_i)$ corresponding to every location a_i is color coded.

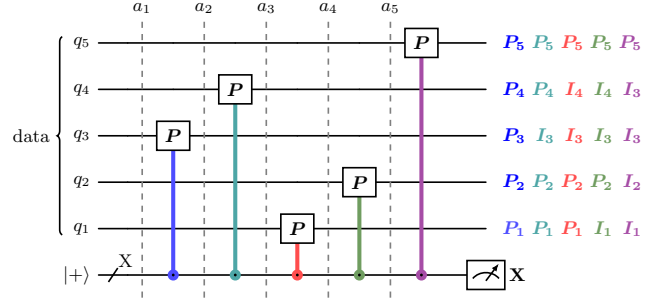


FIG. 3. Due to X error at various positions (a_i) in the ancilla qubit, every hook error $\rho_g(a_i)$ is color-coded accordingly for an ordered stabilizer $g = P_3 P_4 P_1 P_2 P_5$, $P \in \{X, Y, Z\}$.

Now we discuss the two cases of hook errors for circuit-level uncorrelated and correlated hook errors, and show how the correctability of these errors for BACs depends on the weight(w_g) of the stabilizers.

1. Un-correlated errors: Affecting only ancilla qubit

In stabilizer QECCs, it is essential that there are sufficient syndromes available in the lookup table to correct the hook errors propagated through the ancilla qubit during measurement of the syndrome. We count the syndromes in terms of the weight of stabilizers when a single Pauli error occurs on the ancilla qubit during syndrome measurement.

Lemma 1. For any generator $g \in \mathcal{S}$ such that $w_g > 3$ where $g = \prod_i P_{a_i}$ of $[[n, 1, 3]]$ stabilizer QECCs, the number of uncorrectable hook errors satisfies

$$|\mathcal{U}_g| \leq w_g - 3.$$

Proof. Consider the stabilizer generator g with $w_g > 3$ and hook errors $\rho_g(a_1), \rho_g(a_2), \dots, \rho_g(a_{w_g})$ respectively due to errors in locations a_1, a_2, \dots, a_{w_g} . We note that $\rho_g(a_1) = g$ and $\rho_g(a_2) = P_{a_1}$ and $\rho_g(a_{w_g}) = P_{a_{w_g}}$ which

are correctable. The remaining errors have weight at least two. Hence, the number of uncorrectable hook errors is at most $(w_g - 3)$. \square

Corollary 2. Suppose $e_i \in \mathcal{U}_{g_m}$ and $e_j \in \mathcal{U}_{g_t}$ are two different uncorrectable hook errors with the same syndrome occurring in the syndrome of measurement of distinct generators g_m and g_t , respectively. If $e_i e_j \in \mathcal{S}$, then a $[[n, 1, 3]]$ stabilizer QECC can be made fault-tolerant using a look-up table decoder against single-qubit Pauli errors on the ancilla during syndrome extraction, provided

$$S_u \geq \sum_{\substack{g \in \mathcal{S} \\ w_g > 3}} (w_g - 3),$$

where S_u is defined in (5) and w_g is the weight of the stabilizer g .

Proof. From Lemma 1, $|\mathcal{U}_g| \leq w_g - 3$ for each $g \in \mathcal{S}$. Taking the sum of all \mathcal{U}_g over g i.e. $|\mathcal{U}| = \sum_g |\mathcal{U}_g|$. Under the assumption for distinct propagated errors sharing the same syndrome, the decoder must be provided with at least $|\mathcal{U}|$ unique syndromes. Hence

$$|\mathcal{U}| \leq \sum_{\substack{g \in \mathcal{S} \\ w_g > 3}} (w_g - 3),$$

Therefore $|\mathcal{U}|$,

$$S_u \geq \sum_{\substack{g \in \mathcal{S} \\ w_g > 3}} (w_g - 3).$$

\square

This analysis establishes a quantitative relationship between stabilizer weights and the number of syndromes required to correct hook errors due to error in the ancilla qubit, ensuring fault tolerance of the code.

2. Correlated two-qubit gate errors: Affecting data and ancilla both due to two-qubit gates

We now consider correlated errors on the data and ancilla qubits due to a faulty two-qubit gate between the ancilla and data qubit pairs. These faults can introduce arbitrary single-qubit Pauli errors on the data qubits, in addition to Pauli errors in the ancilla qubit. Therefore, these faults generate a larger set of distinct hook errors compared to single-ancilla qubit errors.

Lemma 3. For any generator $g \in \mathcal{S}$ such that $w_g \geq 3$ where $g = \prod_i P_{a_i}$ of $[[n, 1, 3]]$ stabilizer QECCs, every two-qubit depolarizing error due to a fault of an ancilla–data gate during syndrome extraction can potentially produce uncorrectable errors that satisfy

$$|\mathcal{U}_g| \leq 3(w_g - 2).$$

Proof. Consider the stabilizer generator g with $w_g \geq 3$. When a fault occurs in a two-qubit gate between the ancilla and a data qubit, it can cause a two-qubit depolarizing error. As a result, the data qubit coupled to the ancilla may experience any of the three nontrivial Pauli errors $\{X, Y, Z\}$. If the fault happens on the ancilla qubit at any position other than right before the gates corresponding to $C-P_{a_1}$ and $C-P_{a_w}$, the resulting propagated errors can become uncorrectable by a distance-three code. Hence, there are at most $w_g - 2$ such locations per stabilizer. For each location, up to three distinct Pauli errors on the data qubits must be distinguishable by the decoder. Hence, the number of uncorrectable hook errors is at most $3(w_g - 2)$. \square

Corollary 4. Suppose $e_i \in \mathcal{U}_{g_m}$ and $e_j \in \mathcal{U}_{g_t}$ are two different uncorrectable hook errors with the same syndrome occurring in the syndrome of measurement of distinct generators g_m and g_t , respectively. If $e_i e_j \in \mathcal{S}$, then a $[[n, 1, 3]]$ stabilizer QECC is fault-tolerant against depolarizing two-qubit errors due to a fault in two-qubit gates between the ancilla and data qubits provided

$$S_u \geq \sum_{\substack{g \in \mathcal{S} \\ w_g \geq 3}} 3(w_g - 2), \quad (6)$$

where S_u is defined in (5) and w_g is the weight of every stabilizer g .

The proof is similar to the proof of Corollary 2. This result quantifies the additional syndrome requirements for fault-tolerant decoding under correlated two-qubit ancilla-data gate errors.

V. EXPERIMENTAL SETUP

To evaluate and validate the performance of the BACs obtained from graph codes, we perform error rate simulations. The goal is to compare the performance of BACs with that of the flag method. Additionally, we demonstrate how ancilla-induced hook errors impact both total and logical error rates for $[[n, 1, 3]]$ QECCs within a lookup table-based decoding scheme. We calculate the total and logical error rates of given QECCs using CHP (CNOT-Hadamard-Phase) stabilizer simulator [48]. The simulation method is implemented using the Python language. Each trial consists of an initial error correction under random noise, followed by a final noise-free correction using a look-up decoder. Syndrome extraction is repeated up to two times with freshly prepared ancillary qubits. The look-up table is organized into three parts. First, we include syndromes obtained from \mathbf{H}_{xyz} defined as in Eq (4). Second, we add syndromes that arise from errors propagated during syndrome extraction. Lastly, the remaining unmatched syndromes are then assigned to minimum-weight Pauli operators using the parity-check matrix.

A. Error rate calculation

We evaluate both the total and logical error rate for the depolarizing and anisotropic noise with 10^8 trials for each physical error probability. After FT error correction and perfect decoding, each trial is classified according to the residual operator. Total error rate counts all trials in which a nontrivial Pauli error remains on the data qubits, whereas the logical error rate corresponds to the subset of these trials where the residual nontrivial operator anti-commutes with one of the logical operators and commutes with the other one of that QECC. Both rates are obtained as the ratio of the respective counts to the total number of trials.

B. Noise Models

The depolarizing noise model considers the errors occurring in the preparation and measurement steps. Under this model, we account for single-qubit and two-qubit errors occurring on those qubits connected via two-qubit gates. The anisotropic noise models under or over-rotation of the gates in the ion trap qubits [36, 49].

1. Standard Depolarizing Noise Model

The standard depolarizing noise model is commonly used for characterizing physical systems. This model assumes a symmetric depolarization to occur after each quantum gate with a probability p , meaning the quantum state is replaced by the maximally mixed state $I/2$ with probability p , and the state remains unchanged with the complementary probability of $1 - p$.

- **Single-qubit gate errors:** A Pauli error, selected uniformly and independently from $\{X, Y, Z\}$, is drawn with probability p_s after each single-qubit gate. Thus, each of the three errors occurs with probability $p_s/3$.
- **Two-qubit gate errors:** With probability p_t , each two-qubit gate is followed by a two-qubit Pauli error drawn uniformly and independently from the set $\{I, X, Y, Z\} \otimes \{I, X, Y, Z\} \setminus \{I \otimes I\}$. Each of the 15 possible errors occurs with probability $p_t/15$.
- **Measurement errors:** With probability p_m , each single-qubit measurement results in a flipped outcome.
- **State preparation errors:** With probability p_p , the preparation of the $|0\rangle$ state flips to $|1\rangle$ and the preparation of the $|+\rangle$ state flips to $|-\rangle$.

2. Anisotropic Noise Model

The anisotropic noise model includes noise resulting from coupling two-qubit gates on the condition that two-qubit errors will always align with the gates. The simulation of the anisotropic noise model is described as follows:

- **Single-qubit errors, readout errors, and preparation errors:** These errors are applied

with probabilities p_s , p_m , and p_p , respectively, as defined in the standard depolarizing noise model.

- **Two-qubit gate errors:** With probability p_t , each two-qubit controlled-P (CP) gate is followed by a $Z \otimes P$ error. Also, each qubit that has been part of the two-qubit gate will have an independent occurrence of a single-qubit error with p_s .

We analyze various $[[n, 1, 3]]$ QECCs with a bare ancilla qubit. For simplicity each error, p_m , p_p , and p_t is taken to occur with the same probability p_s . A detailed analysis for the $[[6, 1, 3]]$ QECC can be found in Appendix B.

VI. RESULTS

The pseudo-threshold calculation of the $[[n, 1, 3]]$ codes under the bare and flag methods is illustrated in Figure 5. The first column corresponds to the bare scheme, and the second column corresponds to the flag scheme, each evaluated under both anisotropic and depolarizing noise models. In all cases, we plot the logical error rate and total error rate as functions of the physical error rate.

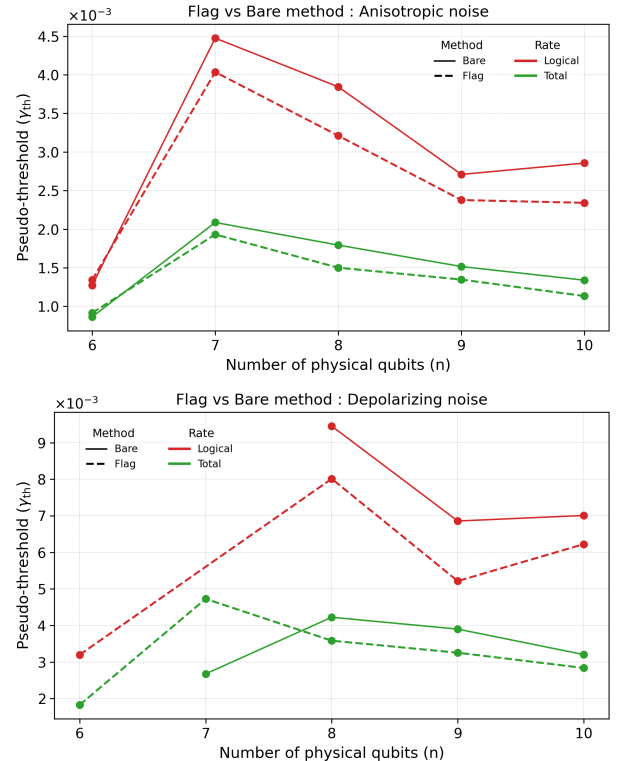


FIG. 4. Comparision of Pseudo-threshold results for $[[n, 1, 3]]$ QECCs between bare and flag method. Note that for depolarizing noise of $[[7, 1, 3]]$ code, the threshold for logical error rate is always less than the physical error rate using the flag method.

In Figure 4, the variation of the pseudo-threshold with the number of physical qubits is shown for codes of fixed distance and one logical qubit. The pseudo-threshold

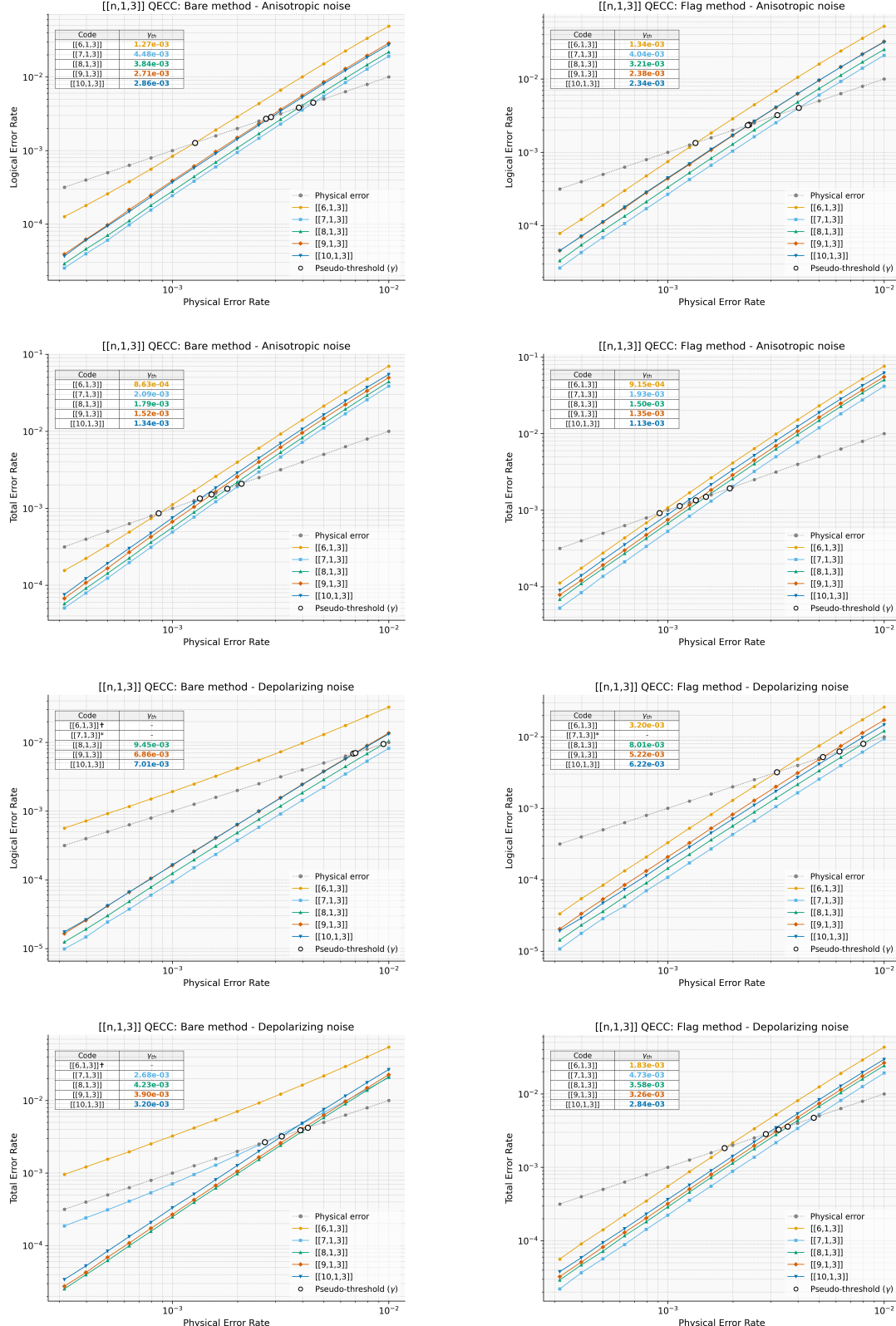


FIG. 5. Pseudo-threshold results for $[[n, 1, 3]]$ QECCs using the bare method and flag method under depolarizing and anisotropic noise.

* – threshold always less than physical error rate in that regime; † – threshold always greater than physical error rate in that regime.

increases till the $[[7, 1, 3]]$ code under anisotropic noise and till the $[[8, 1, 3]]$ code under depolarizing noise for both the bare and flag methods. Notably, no pseudo-threshold is observed for the total error rate in the bare ancilla method for depolarizing noise till the $[[7, 1, 3]]$ codes. This is due to the lack of availability of syndromes to distinguish data errors arising from hook errors. A key observation is that the bare method begins to outperform the flag method from the $[[7, 1, 3]]$ code onward under anisotropic noise, and from the $[[8, 1, 3]]$ code onward under depolarizing noise. These trends indicate that, for distance-three codes with one logical qubit, the $[[8, 1, 3]]$ code provides the most favourable trade-off and can be regarded as the optimal choice under the considered noise models.

VII. CONCLUSION

We have constructed and analyzed a family of $[[n, 1, 3]]$ non-CSS QECCs for $6 \leq n \leq 10$ using graph codes. We demonstrated fault tolerance against hook errors using a single ancilla qubit for syndrome measurement. Our simulations show that for $n \geq 7$, these distance-three codes outperform the flag qubit method under depolarizing noise, while for anisotropic noise, the best-performing codes appear at $n \geq 8$. In contrast, the $[[6, 1, 3]]$ and

$[[7, 1, 3]]$ codes exhibit reduced performance under depolarizing noise when using the bare ancilla method, due to limited syndrome distinguishability of hook errors. Several open directions follow from this work. Extending these constructions to higher distances or multiple logical qubit codes would test the generality of the approach. Since all codes considered here arise from graph code constructions, further exploration of the interplay between graph structures and FT properties could provide new insights into the connections between bare ancilla codes and graph codes. Finally, the bounds we provide on the fault tolerance capabilities of these codes are not tight; therefore, refining them could lead to better code designs.

ACKNOWLEDGMENTS

The authors thank Rahul Garg for his assistance with the proofs and Pranav Maheshwari for his valuable suggestions in preparing this manuscript. R.J. acknowledges funding support from the Department of Science and Technology Grant No. DST/QTC/NQM/QComm/2024/2. H.G. and M.B. thank IISER Bhopal for providing the necessary computational resources and the institute fellowship that supports their doctoral work.

[1] D. Aharonov and M. Ben-Or, [Fault-tolerant quantum computation with constant error](#) (1997).

[2] M. Nielsen and I. Chuang, *Quantum Computation and Quantum Information: 10th Anniversary Edition* (Cambridge University Press, 2010).

[3] C. Vuillot, [Is error detection helpful on IBM 5Q chips ?](#) (2018).

[4] M. Takita, A. W. Cross, A. D. Córcoles, J. M. Chow, and J. M. Gambetta, [Phys. Rev. Lett.](#) **119**, 180501 (2017).

[5] A. M. Steane, [Phys. Rev. Lett.](#) **78**, 2252 (1997).

[6] D. P. DiVincenzo and P. W. Shor, [Phys. Rev. Lett.](#) **77**, 3260 (1996).

[7] E. Knill, [Nature](#) **434**, 39 (2005).

[8] Y. Fujiwara, A. Gruner, and P. Vandendriessche, [IEEE Transactions on Information Theory](#) **61**, 1860 (2015).

[9] Y. Fujiwara, [Phys. Rev. A](#) **90**, 062304 (2014).

[10] T. J. Yoder and I. H. Kim, [Quantum](#) **1**, 2 (2017).

[11] R. Chao and B. W. Reichardt, [Phys. Rev. Lett.](#) **121**, 050502 (2018).

[12] M. Li, M. Gutiérrez, S. E. David, A. Hernandez, and K. R. Brown, [Phys. Rev. A](#) **96**, 032341 (2017).

[13] D. Schlingemann and R. F. Werner, [Physical Review A](#) **65**, 10.1103/physreva.65.012308 (2001).

[14] M. Van den Nest, J. Dehaene, and B. De Moor, [Phys. Rev. A](#) **69**, 022316 (2004).

[15] C. Cafaro, D. Markham, and P. van Loock, [Physical Review A](#) (2015).

[16] D. Schlingemann, [Stabilizer codes can be realized as graph codes](#) (2001), [arXiv:quant-ph/0111080 \[quant-ph\]](#).

[17] P. W. Shor, [Phys. Rev. A](#) **52**, R2493 (1995).

[18] A. M. Steane, [Phys. Rev. A](#) **54**, 4741 (1996).

[19] R. Laflamme, C. Miquel, J. P. Paz, and W. H. Zurek, [Phys. Rev. Lett.](#) **77**, 198 (1996).

[20] D. Gottesman, [Stabilizer codes and quantum error correction](#) (1997), [arXiv:quant-ph/9705052 \[quant-ph\]](#).

[21] A. R. Calderbank and P. W. Shor, [Physical Review A](#) **54**, 1098 (1996).

[22] D. Maurice, J.-P. Tillich, and I. Andriyanova, in [2013 IEEE International Symposium on Information Theory](#) (2013) pp. 907–911.

[23] E. Dennis, A. Kitaev, A. Landahl, and J. Preskill, [Journal of Mathematical Physics](#) **43**, 4452 (2002).

[24] A. Ashikhmin, C.-Y. Lai, and T. A. Brun, in [2014 IEEE International Symposium on Information Theory](#) (2014) pp. 546–550.

[25] D. Crow, R. Joynt, and M. Saffman, [Phys. Rev. Lett.](#) **117**, 130503 (2016).

[26] V. N. Premakumar, H. Sha, D. Crow, E. Bach, and R. Joynt, [Quantum Information Processing](#) **20**, 84 (2021).

[27] E. Guttentag, A. Nemec, and K. R. Brown, in [2024 IEEE International Symposium on Information Theory \(ISIT\)](#) (2024) pp. 2281–2286.

[28] C. Chamberland and M. E. Beverland, [Quantum](#) **2**, 53 (2018).

[29] R. Chao and B. W. Reichardt, [PRX Quantum](#) **1**, 010302 (2020).

[30] D. M. Debroy and K. R. Brown, [Phys. Rev. A](#) **102**, 052409 (2020).

- [31] D. Bhatnagar, M. Steinberg, D. Elkouss, C. G. Almudever, and S. Feld, in *2023 IEEE International Conference on Quantum Computing and Engineering (QCE)*, Vol. 01 (2023) pp. 63–69.
- [32] B. Anker and M. Marvian, *PRX QUANTUM* **5**, 10.1103/PRXQuantum.5.040340 (2024).
- [33] Y. Takada and K. Fujii, *PRX QUANTUM* **5**, 10.1103/PRXQuantum.5.030352 (2024).
- [34] B. Pato, T. Tansuwanont, S. Huang, and K. R. Brown, *PRX Quantum* **5**, 020336 (2024).
- [35] L. Lao and C. G. Almudever, *Phys. Rev. A* **101**, 032333 (2020).
- [36] P. Parrado-Rodríguez, C. Ryan-Anderson, A. Bermudez, and M. Müller, *Quantum* **5**, 487 (2021).
- [37] M. Li, D. Miller, and K. R. Brown, *Phys. Rev. A* **98**, 050301 (2018).
- [38] S. Huang and K. R. Brown, *Phys. Rev. A* **101**, 042312 (2020).
- [39] P. Maheshwari and A. Raina, in *2024 IEEE International Symposium on Information Theory Workshops (ISIT-W)* (2024) pp. 1–6.
- [40] R. Raussendorf, D. E. Browne, and H. J. Briegel, *Phys. Rev. A* **68**, 022312 (2003).
- [41] A. Patil and S. Guha, Clifford manipulations of stabilizer states: A graphical rule book for clifford unitaries and measurements on cluster states, and application to photonic quantum computing (2023), arXiv:2312.02377.
- [42] M. Hein, J. Eisert, and H. J. Briegel, *Phys. Rev. A* **69**, 062311 (2004).
- [43] M. Grassl, in *Coding and Cryptology*, edited by Y. M. Chee, Z. Guo, S. Ling, F. Shao, Y. Tang, H. Wang, and C. Xing (Springer Berlin Heidelberg, 2011) pp. 142–158.
- [44] M. Grassl, A. Klappenecker, and M. Rötteler, in *Proceedings IEEE International Symposium on Information Theory*, (2002) pp. 45–.
- [45] D. Schlingemann, *Stabilizer codes can be realized as graph codes* (2001).
- [46] Y. Hwang and J. Heo, *Quantum Info. Comput.* **16**, 237–250 (2016).
- [47] P. J. Nadkarni, A. Raina, and S. G. Srinivasa, in *2017 IEEE Globecom Workshops (GC Wkshps)* (2017) pp. 1–6.
- [48] S. Aaronson and D. Gottesman, *Phys. Rev. A* **70**, 052328 (2004).
- [49] A. Sørensen and K. Mølmer, *Phys. Rev. Lett.* **82**, 1971 (1999).

Appendix A: MBQC Encoding

A graph state can be mathematically represented as an undirected graph $G = (V, E)$, where V denotes the set of vertices corresponding to the qubits, and E represents the edges corresponding to CZ gates between the qubits. And all the CZ gates connected with a vertex i can be written as:

$$\prod_{(i,j) \in E_i} \text{CZ}_{ji} = \prod_{j \in \mathcal{N}_i} I_j \otimes |0\rangle\langle 0|_i + \prod_{j \in \mathcal{N}_i} Z_j \otimes |1\rangle\langle 1|_i \quad (\text{A1})$$

where E_i represents the set of all edges connected to node i and \mathcal{N}_i the set of all neighboring nodes of node $i \in V$.

Proof. Consider a state $|\psi_m\rangle$, an n -qubit cluster with one message qubit i .e. $|\phi_m\rangle = \alpha|0\rangle_m + \beta|1\rangle_m$, where $m = n+1$.

$$\begin{aligned} |\psi_m\rangle &= \prod_{i \in \{1, 2, \dots, n\}} \prod_{\substack{(i,j) \in E_i \\ j > i}} \text{CZ}_{ij} \left(|+\rangle^{\otimes n} |\phi_m\rangle \right) \\ &= \left(\prod_{i \in \{1, 2, \dots, n\}} \prod_{\substack{(i,j) \in E_i \setminus E_m \\ j > i}} \text{CZ}_{ij} \left(\prod_{\substack{(m,k) \in E_m \\ k \in \{1, 2, \dots, n\}}} \text{CZ}_{mk} \left(|+\rangle^{\otimes n} |\phi_m\rangle \right) \right) \right) \\ &\quad \text{where } E_m \text{ represents the set of all the edges connected to the message qubit and using Eq.(A1), we get} \\ &= \left(\prod_{i \in \{1, 2, \dots, n\}} \prod_{\substack{(i,j) \in E_i \setminus E_m \\ j > i}} \text{CZ}_{ij} \right) \left[\left(\prod_{k \in \mathcal{N}_m} I_k \otimes |0\rangle\langle 0|_m + \prod_{k \in \mathcal{N}_m} Z_k \otimes |1\rangle\langle 1|_m \right) |+\rangle^{\otimes n} |\phi_m\rangle \right] \\ &= \left(\prod_{i \in \{1, 2, \dots, n\}} \prod_{\substack{(i,j) \in E_i \setminus E_m \\ j > i}} \text{CZ}_{ij} \right) \left[\alpha |+\rangle^{\otimes n} |0\rangle_m + \right. \\ &\quad \left. \beta \prod_{k \in \mathcal{N}_m} Z_k |+\rangle^{\otimes n} |1\rangle_m \right] \\ &= \alpha U |+\rangle^{\otimes n} |0\rangle_m + \beta U \prod_{k \in \mathcal{N}_m} Z_k |+\rangle^{\otimes n} |1\rangle_m, \\ &\quad \text{where } U = \prod_{i \in \{1, 2, \dots, n\}} \prod_{\substack{(i,j) \in E_i \setminus E_m \\ j > i}} \text{CZ}_{ij}. \\ &= \alpha |G\rangle |0\rangle_m + \beta \prod_{k \in \mathcal{N}_m} Z_k |G\rangle |1\rangle_m, \\ &\quad \text{where } |G\rangle = U |+\rangle^{\otimes n}. \end{aligned}$$

Hence

$$|\psi\rangle = \left(\alpha|G\rangle + \beta \prod_{k \in \mathcal{N}_m} Z_k|G\rangle \right) \frac{|+\rangle_m}{2} + \left(\alpha|G\rangle - \beta \prod_{k \in \mathcal{N}_m} Z_k|G\rangle \right) \frac{|-\rangle_m}{2}.$$

After the measurement of the message qubit in a X basis we will get the encoded state in $\alpha|G\rangle + (-1)^p \beta \prod_{k \in \mathcal{N}_m} Z_k|G\rangle$ form, where p will be mapped to 0 and 1 for the outcomes $|+\rangle_m$ and $|-\rangle_m$ respectively. \square

Appendix B: [[6, 1, 3]] Bare code construction

For the construction of the [[6, 1, 3]] bare code, we first consider a six-qubit graph state with one message qubit. The message qubit is also connected with CZ gates. Hence, the first six qubits, namely those labeled 0 through 5, are prepared in the $|+\rangle$ state, and the seventh qubit, labeled 6, is the message qubit as seen in Figure 6.

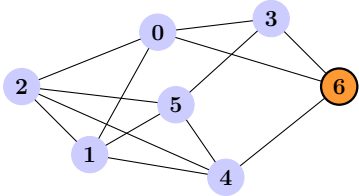


FIG. 6. Six qubit graph state with one message qubit (orange) which is measured in the X basis.

\hat{S}_6 is the stabilizer for the above state with generators:

$$\hat{S}_6 = \langle X_0 Z_1 Z_2 Z_3 Z_6, Z_0 X_1 Z_2 Z_4 Z_5, Z_0 Z_1 X_2 Z_4 Z_5, Z_0 X_3 Z_5 Z_6, Z_1 Z_2 X_4 Z_5 Z_6, Z_1 Z_2 Z_3 Z_4 X_5 \rangle. \quad (\text{B1})$$

Once the message qubit is measured in the X basis, the corresponding logical information is encoded into the rest of the qubits. Then, with the help of Algorithm 1, the stabilizers of the encoded state are found, which are defined in Eq. (B2).

$$S_6 = \langle Z_0 X_1 Z_2 Z_4 Z_5, Z_0 Z_1 X_2 Z_4 Z_5, Y_0 Z_1 Z_2 Y_3 Z_5, X_0 Z_3 X_4 Z_5, Z_1 Z_2 Z_3 Z_4 X_5 \rangle. \quad (\text{B2})$$

The corresponding logical operators are $X_l = Z_0 X_3 Z_5$, $Z_l = Z_0 Z_3 Z_4$.

Using Algorithm 2, we obtained the rearranged operators for every stabilizer generator, such that due to the hook errors in the bare ancilla qubit, the propagated errors have unique syndromes as mentioned in the yellow box, given in the Table III. We note that the [[6, 1, 3]] code is immune to single-qubit error in data qubits or an ancilla qubit, but not all the two-qubit errors due to syndrome

unavailability. A total of $2^{n-k} - 1 = 31$ non-zero five-bit tuples are available to detect the errors in data qubits. Seventeen are utilised for single-qubit errors mentioned in Table I. Manually, we assign nine syndromes arising from the ancilla qubit to the data qubits as detailed in Table III. Three syndromes are assigned for three specific hook errors, and two syndromes are assigned for two random two-qubit data errors as seen in Table II. Hence, the lookup table has been meticulously designed by manually associating each syndrome with specific errors. Similarly, all the $[[n, 1, 3]]$ QECCs are done where $n \in \{6, 7, 8, 9, 10\}$ provided in supplement material.

Error	Syndrome	Error	Syndrome	Error	Syndrome
Z_0	00110	X_0	11100	Y_0	11010
Z_1	10000	X_1	01101	Y_1	11101
Z_2	01000	X_2	10101	Y_2	11101
Z_3	00100	X_3	00111	Y_3	00011
Z_4	00010	X_4	11001	Y_4	11011
Z_5	00001	X_5	11110	Y_5	11111

TABLE I. Syndrome table for the [[6, 1, 3]] bare code.

LOOK-UP TABLE with manual entries		
Syndrome	Error	Location
01100	$X_1 Z_5$	$Y_0 Z_1 Z_2 Y_3 Z_5$
01111	$Z_1 Y_5$	$Z_1 Z_2 Z_3 Z_4 X_5$
10111	$X_2 Z_4$	$Z_1 Z_2 Z_3 Z_4 X_5$
00101	$Z_2 Z_5$	Two qubit data error
10011	$Z_2 Z_4$	Two qubit data error

TABLE II. Lookup table used in the correction of errors on the data qubits of the [[6, 1, 3]] code.

Data Error	Syndrome	Data Error	Syndrome
$Z_0X_1Z_2Z_4Z_5 \longrightarrow Z_0X_1Z_4Z_2Z_5$			
Z_0X_1	01011	Z_0Y_1	11011
Z_0Z_1	10110	$Z_0X_1X_4$	10010
$Z_0X_1Y_4$	10000	Z_2Z_5	01001
Y_2Z_5	11100	X_2Z_5	10100
$Z_0Z_1X_2Z_4Z_5 \longrightarrow Z_0Z_1Z_4X_2Z_5$			
Z_0X_1	01011	Z_0Y_1	11011
Z_0Z_1	10110	$Z_0Z_1X_4$	01111
$Z_0Z_1Y_4$	01101	X_2Z_5	10100
Z_2Z_5	01001	Y_2Z_5	11100
$Y_0Z_1Z_2Y_3Z_5 \longrightarrow Y_0Z_2Y_3Z_1Z_5$			
Y_0X_2	01111	Y_0Y_2	00111
Y_0Z_2	10010	$Y_0Z_2X_3$	10101
Z_1Z_5	10001	$Y_0Z_2Z_3$	10110
Y_1Z_5	11100	X_1Z_5	01100
$X_0Z_3X_4Z_5 \longrightarrow X_0Z_3X_4Z_5$			
X_0X_3	11011	X_0Y_3	11111
X_0Z_3	11000	Z_4Z_5	00011
Y_4Z_5	11010	Z_5	00001
$Z_1Z_2Z_3Z_4X_5 \longrightarrow Z_1X_5Z_3Z_2Z_4$			
Z_1X_5	01110	Z_1Y_5	01111
Z_1Z_5	10001	$Z_1X_5X_3$	01001
$Z_1X_5Y_3$	01101	Z_2Z_4	01010
Y_2Z_4	11111	X_2Z_4	10111

TABLE III. Propagated errors in the $[[6, 1, 3]]$ code with their syndromes for the corresponding stabilizers. The rearranging of stabilizers is illustrated in grey boxes. The yellow coloured box represents the error generated by a fault in the bare ancilla qubit. Red colour errors are logical errors due to hook errors, whereas black coloured errors are correctable.

Supplemental Material: Fault-tolerant syndrome extraction in $[[n, 1, 3]]$ non-CSS code family generated using measurements on graph states

Appendix C: Introduction

For the bare code construction, we specify the reordered stabilizers used for the corresponding quantum error-correcting code. The resource state consists of $(n + 1)$ qubits: an n -qubit graph state together with an additional message qubit. Measuring the message qubit in the X basis teleports its state into the n graph qubits, thereby preparing the $[[n, 1, 3]]$ graph code. We use Algorithm 3 for the lookup table construction. The lookup table of syndromes used for decoding is organized into three parts. First, we include syndromes obtained from the modified parity-check matrix, defined as

$$\mathbf{H}_{xyz} = [\mathbf{H}_x \mid \mathbf{H}_z \mid \mathbf{H}_x \oplus \mathbf{H}_z].$$

Second, we add syndromes that arise from errors propagated during syndrome extraction. Finally, the remaining syndromes that do not fall into the above categories are paired with their corresponding minimum-weight error operators.

Algorithm 3: Permutation-based construction of stabilizer syndromes

Input: A stabilizer $g = [(q_1, P_1), \dots, (q_w, P_w)]$ with $w > 2$, q is qubit location and $P \in \{X, Y, Z\}$

Output: Maps $\{\text{orgComb}, \text{allComb}\}$ indexed by permutations of g

```

1 Form  $\mathbf{H}_{xyz} \leftarrow [\mathbf{H}_x \mid \mathbf{H}_z \mid \mathbf{H}_x \oplus \mathbf{H}_z]$ ;
2 Initialize empty maps  $\text{orgComb}$ ,  $\text{allComb}$ ;
3 foreach permutation  $\tilde{g} = [(q_{\pi(1)}, P_{\pi(1)}), \dots, (q_{\pi(w)}, P_{\pi(w)})]$  of  $g$  do
4   Set prefix  $\gamma \leftarrow [(q_{\pi(1)}, P_{\pi(1)})]$ ;
5    $c \leftarrow \text{col}(\mathbf{H}_{xyz}, q_{\pi(1)}, P_{\pi(1)})$ ;
6   Initialize empty sets  $\text{exOrg}$ ,  $\text{exAll}$ ;
7   for  $i = 2$  to  $w - 1$  do
8     Let  $(q, P_{\text{orig}}) \leftarrow (q_{\pi(i)}, P_{\pi(i)})$ ;
9     foreach  $P \in \{X, Y, Z\}$  do
10       if  $i = w - 1 \wedge P = P_{\text{orig}}$  then
11          $\quad$  skip
12          $c' \leftarrow (c + \text{col}(\mathbf{H}_{xyz}, q, P)) \bmod 2$ ;
13         if  $c' = 0 \vee c' \in \{\sigma : (\_, \sigma) \in \text{exAll}\}$  then
14            $\quad$  discard  $\tilde{g}$ 
15         Insert  $(\gamma \cup \{(q, P)\}, c')$  into  $\text{exAll}$ ;
16         if  $P = P_{\text{orig}}$  then
17            $\quad$  Insert  $(\gamma \cup \{(q, P_{\text{orig}})\}, c')$  into  $\text{exAll}$ ;
18          $c \leftarrow (c + \text{col}(\mathbf{H}_{xyz}, q, P_{\text{orig}})) \bmod 2$ ;
19          $\gamma \leftarrow \gamma \cup \{(q, P_{\text{orig}})\}$ ;
20    $\text{orgComb}[\tilde{g}] \leftarrow \text{exOrg}$ ,  $\text{allComb}[\tilde{g}] \leftarrow \text{exAll}$ ;
21 return  $\text{orgComb}$ ,  $\text{allComb}$ ;
22 Note:  $\text{col}(\mathbf{H}_{xyz}, q, P)$  represents the syndrome of operator  $P$  at qubit location  $q$ .

```

Appendix D: Code Details

1. $[[6, 1, 3]]$ code

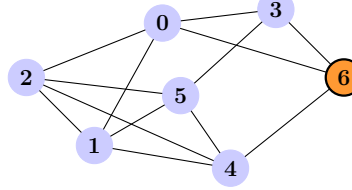


FIG. S1. Six qubit graph state(blue) with one message qubit(orange).

Stabilizer generating set:

$$\langle Z_0X_1Z_2Z_4Z_5, \quad Z_0Z_1X_2Z_4Z_5, \quad Y_0Z_1Z_2Y_3Z_5, \quad X_0Z_3X_4Z_5, \quad Z_1Z_2Z_3Z_4X_5 \rangle$$

Logical operators:

$$X_l = Z_0X_3Z_5, \quad Z_l = Z_0Z_3Z_4.$$

Error (Z)	Syndrome (Z)	Error (X)	Syndrome (X)	Error (Y)	Syndrome (Y)
Z_0	00110	X_0	11100	Y_0	11010
Z_1	10000	X_1	01101	Y_1	11101
Z_2	01000	X_2	10101	Y_2	11101
Z_3	00100	X_3	00111	Y_3	00011
Z_4	00010	X_4	11001	Y_4	11011
Z_5	00001	X_5	11110	Y_5	11111

TABLE I. Single-qubit error syndromes for the $[[6, 1, 3]]$ code

$Z_0X_1Z_2Z_4Z_5$ $\rightarrow Z_0X_1Z_4Z_2Z_5$		$Z_0Z_1X_2Z_4Z_5$ $\rightarrow Z_0Z_1Z_4X_2Z_5$		$Y_0Z_1Z_2Y_3Z_5$ $\rightarrow Y_0Z_2Y_3Z_1Z_5$		$X_0Z_3X_4Z_5$ $\rightarrow X_0Z_3X_4Z_5$		$Z_1Z_2Z_3Z_4X_5$ $\rightarrow Z_1X_5Z_3Z_2Z_4$	
Error	Syndrome	Error	Syndrome	Error	Syndrome	Error	Syndrome	Error	Syndrome
Z_0X_1	01011	Z_0X_1	01011	Y_0X_2	01111	X_0Y_3	11111	Z_1X_5	01110
Z_0Y_1	11011	Z_0Y_1	11011	Y_0Y_2	00111	X_0Z_3	11000	Z_1Y_5	01111
Z_0Z_1	10110	Z_0Z_1	10110	Y_0Z_2	10010	Z_4Z_5	00011	Z_1Z_5	10001
$Z_0X_1X_4$	10010	$Z_0Z_1X_4$	01111	$Y_0Z_2X_3$	10101	Y_4Z_5	11010	$Z_1X_5X_3$	01001
$Z_0X_1Y_4$	10000	$Z_0Z_1Y_4$	01101	Z_1Z_5	10001	X_0X_3	11011	$Z_1X_5Y_3$	01101
Z_2Z_5	01001	X_2Z_5	10100	$Y_0Z_2Z_3$	10110	—	—	Z_2Z_4	01010
Y_2Z_5	11100	Z_2Z_5	01001	Y_2Z_5	11100	—	—	Y_2Z_4	11111
X_2Z_5	10100	Y_1Z_5	11100	X_1Z_5	01100	—	—	X_2Z_4	10111

TABLE II. Propagated errors in the $[[6, 1, 3]]$ code with their syndromes under reordering stabilizers.

Error	Syndrome
Z_3Z_5	00101
Z_2Y_4	10011

TABLE III. Left-alone syndromes used in the lookup table.

2. $[[7, 1, 3]]$ code

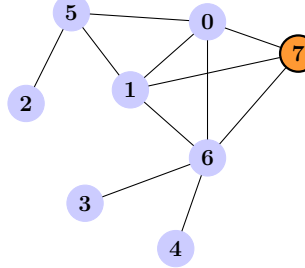


FIG. S2. Seven qubit graph state(blue) with one message qubit(orange).

Stabilizer generating set:

$$\langle X_0X_1, X_2Z_5, X_3Z_6, X_4Z_6, Z_0Z_1Z_2X_5, Y_0Z_1Z_3Z_4Z_5Y_6 \rangle$$

Logical operators:

$$X_l = X_0Z_5Z_6, \quad Z_l = Z_0Z_1Z_6.$$

Error (Z)	Syndrome (Z)	Error (X)	Syndrome (X)	Error (Y)	Syndrome (Y)
Z_0	100001	X_0	000011	Y_0	100010
Z_1	100000	X_1	000011	Y_1	100011
Z_2	010000	X_2	000010	Y_2	010010
Z_3	001000	X_3	000001	Y_3	001001
Z_4	000100	X_4	000001	Y_4	000101
Z_5	000010	X_5	010001	Y_5	010011
Z_6	000001	X_6	001101	Y_6	001100

TABLE IV. Single-qubit error syndromes for the $[[7, 1, 3]]$ code.

$Z_0Z_1Z_2X_5 \rightarrow Z_0Z_2Z_1X_5$		$Y_0Z_1Z_3Z_4Z_5Y_6 \rightarrow Y_0Z_3Z_1Z_4Z_5Y_6$	
Error	Syndrome	Error	Syndrome
Z_0Z_2	110001	Y_0X_3	100011
Y_1X_5	110010	Y_0Y_3	101011
X_1X_5	010010	Y_0Z_3	101010
Z_0X_2	100011	$Y_0Z_3X_1$	101001
Z_0Y_2	110011	$Y_0Z_3Y_1$	001001
—	—	$Y_0Z_3Z_1$	001010
—	—	$Y_4Z_5Y_6$	001011
—	—	$X_4Z_5Y_6$	001111
—	—	Z_5Y_6	001110
—	—	Y_5Y_6	011111
—	—	X_5Y_6	011101

TABLE V. Propagated errors in the $[[7, 1, 3]]$ code with their syndromes for the corresponding reordering stabilizers.

Error	Syndrome	Error	Syndrome	Error	Syndrome
$Z_1 Z_2 Z_4$	110100	$Z_2 Y_6$	011100	$Z_4 Z_5$	000110
$Y_4 Z_5$	000111	$Y_1 Y_6$	101111	$Y_0 Y_6$	101110
$Z_2 Z_3$	011000	$Z_2 Z_4$	010100	$Y_2 Y_6$	011110
$Z_1 Z_2$	110000	$Y_1 Z_4$	100111	$Y_0 Z_4$	100110
$Z_3 Y_5$	011011	$Z_4 Y_5$	010111	$Y_2 Z_3$	011010
$Y_2 Z_4$	010110	$Z_1 Y_6$	101100	$Z_0 Y_6$	101101
$Z_2 Y_3$	011001	$Z_2 Y_4$	010101	$Z_1 Z_3$	101000
$Z_1 Z_4$	100100	$Z_0 Z_4$	100101	$Z_1 Y_2 Y_6$	111110
$Z_1 Y_5 Y_6$	111111	$Z_0 Z_2 Y_6$	111101	$Z_0 Z_3 Y_5$	111010
$Z_0 Z_4 Y_5$	110110	$Z_1 Z_2 Y_6$	111100	$Z_1 Z_3 Y_5$	111011
$Z_1 Z_4 Y_5$	110111	$Z_0 Z_2 Z_3$	111001	$Z_0 Z_2 Z_4$	110101
$Z_1 Z_2 Z_3$	111000	—	—	—	—

TABLE VI. Left-alone syndromes used in the lookup table for the $[[7, 1, 3]]$ code.

3. $[[8, 1, 3]]$ code

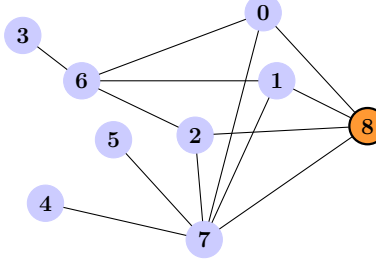


FIG. S3. Eight qubit graph state(blue) with one message qubit(orange).

Stabilizer generating set:

$$\langle X_0X_1, X_0X_2, X_3Z_6, X_4Z_7, X_5Z_7, Z_0Z_1Z_2Z_3X_6, Y_0Z_1Z_2Z_4Z_5Z_6Y_6 \rangle$$

Logical operators:

$$X_l = X_0Z_6Z_7, \quad Z_l = Z_0Z_1Z_2Z_7.$$

Error (Z)	Syndrome (Z)	Error (X)	Syndrome (X)	Error (Y)	Syndrome (Y)
Z_0	1100001	X_0	0000011	Y_0	1100010
Z_1	1000000	X_1	0000011	Y_1	1000011
Z_2	0100000	X_2	0000011	Y_2	0100011
Z_3	0010000	X_3	0000010	Y_3	0010010
Z_4	0001000	X_4	0000001	Y_4	0001001
Z_5	0000100	X_5	0000001	Y_5	0000101
Z_6	0000010	X_6	0010001	Y_6	0010011
Z_7	0000001	X_7	0001101	Y_7	0001100

TABLE VII. Single-qubit error syndromes for the $[[8, 1, 3]]$ code

$Z_0Z_1Z_2Z_3X_6 \rightarrow Z_0Z_3Z_1X_6Z_2$		$Y_0Z_1Z_2Z_4Z_5Z_6Y_7 \rightarrow Z_1Z_4Y_0Z_5Z_6Y_7Z_2$	
Error	Syndrome	Error	Syndrome
Z_0Z_3	1110001	Z_1Z_4	1001000
Z_2X_6	0110001	$Z_1Z_4Y_0$	0101010
Z_0X_3	1100011	$Z_2Z_6Y_7$	0101110
Z_0Y_3	1110011	Z_2Y_7	0101100
$Z_0Z_3X_1$	1110010	Z_1X_4	1000001
$Z_0Z_3Y_1$	0110010	Z_1Y_4	1001001
Z_2X_6	0110001	$Z_1Z_4X_0$	1001011
Z_2Y_6	0110011	$Z_1Z_4Z_0$	0101001
—	—	$Z_1Z_4Y_0X_5$	0101011
—	—	$Z_1Z_4Y_0Y_5$	0101111
—	—	$Z_2Y_6Y_7$	0111111
—	—	$Z_2X_6Y_7$	0111101
—	—	Z_2Z_7	0100001
—	—	Z_2X_7	0101101

TABLE VIII. Propagated errors in the $[[8, 1, 3]]$ code with their syndromes under reordering stabilizers.

Error	Syndrome	Error	Syndrome	Error	Syndrome
$Z_2Y_3Z_5$	0110110	Z_6Y_7	0001110	Z_6X_7	0001111
Z_3Y_7	0011100	Z_4Z_6	0001010	Z_5Z_6	0000110
Y_4Z_6	0001011	Y_5Z_6	0000111	Z_3X_7	0011101
Z_1Z_2	1100000	Y_0X_7	1101111	Z_1Z_6	1000010
Z_1Y_3	1010010	Y_1X_7	1001110	Y_6Y_7	0011111
Z_3Z_4	0011000	Z_3Z_5	0010100	Y_3Y_7	0011110
Z_0X_6	1110000	Y_0Y_4	1101011	Y_0Y_5	1100111
Y_0Y_7	1101110	Z_1X_6	1010001	Y_1Y_4	1001010
Y_1Y_5	1000110	Z_1Z_3	1010000	Y_1Y_7	1001111
Y_2Y_5	0100110	Z_2Z_3	0110000	Z_4Y_6	0011011
Z_5Y_6	0010111	Y_3Z_4	0011010	Y_3Z_5	0010110
Y_0Z_4	1101010	Y_0Z_5	1100110	Z_1Y_6	1010011
Y_1Z_5	1000111	Y_2Z_5	0100111	Z_0X_7	1101100
Z_1X_7	1001101	Z_3Y_4	0011001	Z_3Y_5	0010101
Z_0Y_4	1101000	Z_0Y_5	1100100	Z_0Y_7	1101101
Z_1Y_5	1000101	Z_1Y_7	1001100	Z_2Y_5	0100101
Z_0Z_4	1101001	Z_0Z_5	1100101	Z_1Z_5	1000100
Z_2Z_4	0101000	Z_2Z_5	0100100	$Z_0Y_6Y_7$	1111110
$Z_1Y_6Y_7$	1011111	$Z_0Y_3Y_7$	1111111	$Z_1Y_3Y_7$	1011110
$Z_2Y_3Y_7$	0111110	$Z_0Z_3Y_7$	1111101	$Z_0Z_4Y_6$	1111010
$Z_0Z_5Y_6$	1110110	$Z_0Z_3X_7$	1111100	$Z_1Z_3Y_7$	1011100
$Z_1Z_4Y_6$	1011011	$Z_1Z_5Y_6$	1010111	$Z_1Z_3X_7$	1011101
$Z_2Z_3Y_7$	0111100	$Z_2Z_4Y_6$	0111011	$Z_2Z_5Y_6$	0110111
$Z_0Z_3Z_4$	1111001	$Z_0Z_3Z_5$	1110101	$Z_0Z_3Y_4$	1111000
$Z_0Z_3Y_5$	1110100	$Z_1Z_3Z_4$	1011000	$Z_1Z_3Z_5$	1010100
$Z_1Z_3Y_4$	1011001	$Z_1Z_3Y_5$	1010101	$Z_2Z_3Z_4$	0111000
$Z_2Z_3Z_5$	0110100	$Z_2Z_3Y_4$	0111001	$Z_2Z_3Y_5$	0110101
$Z_0Y_3Z_4$	1111011	$Z_0Y_3Z_5$	1110111	$Z_1Y_3Z_4$	1011010
$Z_1Y_3Z_5$	1010110	$Z_2Y_3Z_4$	0111010	—	—

TABLE IX. Left-alone syndromes used in the lookup table for the $[[8, 1, 3]]$ code.

4. $[[9, 1, 3]]$ code

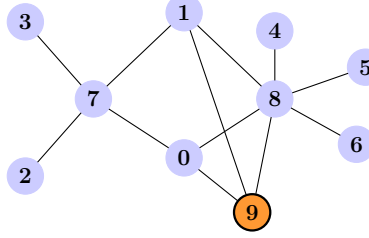


FIG. S4. Nine qubit graph state(blue) with one message qubit(orange).

Stabilizer generating set:

$$\langle X_0X_1, X_2Z_7, X_3Z_7, X_4Z_8, X_5Z_8, X_6Z_8, Z_0Z_1Z_2Z_3X_7, Y_0Z_1Z_4Z_5Z_6Z_7Y_8 \rangle$$

Logical operators:

$$X_l = X_0Z_7Z_8, \quad Z_l = Z_0Z_1Z_8.$$

Error (Z)	Syndrome (Z)	Error (X)	Syndrome (X)	Error (Y)	Syndrome (Y)
Z_0	10000001	X_0	00000011	Y_0	10000010
Z_1	10000000	X_1	00000011	Y_1	10000011
Z_2	01000000	X_2	00000010	Y_2	01000010
Z_3	00100000	X_3	00000010	Y_3	00100010
Z_4	00010000	X_4	00000001	Y_4	00010001
Z_5	00001000	X_5	00000001	Y_5	00001001
Z_6	00000100	X_6	00000001	Y_6	00000101
Z_7	00000010	X_7	01100001	Y_7	01100011
Z_8	00000001	X_8	00011101	Y_8	00011100

TABLE X. Single-qubit error syndromes for the $[[9, 1, 3]]$ code

$Z_0Z_1Z_2Z_3X_7 \rightarrow Z_2Z_0Z_3Z_1X_7$		$Y_0Z_1Z_4Z_5Z_6Z_7Y_8 \rightarrow Z_4Y_0Z_5Z_1Z_6Z_7Y_8$	
Error	Syndrome	Error	Syndrome
Z_2X_0	01000011	Z_7Y_8	00011110
Z_2Y_0	11000010	$Z_6Z_7Y_8$	00011010
Z_2Z_0	11000001	Z_4X_0	00010011
$Z_2Z_0X_3$	11000011	Z_4Y_0	10010010
$Z_2Z_0Y_3$	11100011	Z_4Z_0	10010001
Z_1X_7	11100001	$Z_4Y_0X_5$	10010011
Y_1X_7	11100010	$Z_4Y_0Y_5$	10011011
X_1X_7	01100010	$Z_4Y_0Z_5$	10011010
—	—	$Z_4Y_0Z_5X_1$	10011001
—	—	$Z_4Y_0Z_5Y_1$	00011001
—	—	$Y_6Z_7Y_8$	00011011
—	—	$X_6Z_7Y_8$	00011111
—	—	Y_7Y_8	01111111
—	—	X_7Y_8	01111101

TABLE XI. Propagated errors in the $[[9, 1, 3]]$ code with their syndromes under reordering stabilizers.

TABLE XII. Syndrome table for errors

Error	Syndrome	Error	Syndrome	Error	Syndrome	Error	Syndrome
$Z_0Y_3Z_4Z_5$	10111011	Z_2Z_3	01100000	X_7X_8	01111100	Z_2Z_8	01000001
Z_3Z_8	00100001	Z_4Z_7	00010010	Z_5Z_7	00001010	Z_6Z_7	00000110
Y_5Z_7	00001011	Y_6Z_7	00000111	Z_2Y_7	00100011	Y_1Y_8	10011111
Y_0Y_8	10011110	Y_2X_8	01011111	Y_3X_8	00111111	Y_4X_7	01110000
Z_5Z_6	00001100	Y_5X_7	01101000	Z_4Z_6	00010100	Y_6X_7	01100100
Z_4Z_5	00011000	Y_7X_8	01111110	Z_1Z_2	11000000	Z_1Z_3	10100000
Y_1Z_5	10001011	Y_1Z_6	10000111	Z_0Z_3	10100001	Y_0Z_5	10001010
Y_0Z_6	10000110	Z_0X_7	11100000	Y_2Y_4	01010011	Y_2Y_5	01001011
Y_2Y_6	01000111	Y_2Y_8	01011110	Y_3Y_4	00110011	Y_3Y_5	00101011
Y_3Y_6	00100111	Y_3Y_8	00111110	Y_4Y_7	01110010	Z_5Y_6	00001101
Y_5Y_7	01101010	Z_4Y_6	00010101	Y_6Y_7	01100110	Z_1Y_3	10100010
Z_0Y_3	10100011	Y_2Z_4	01010010	Y_2Z_5	01001010	Y_2Z_6	01000110
Y_3Z_4	00110010	Y_3Z_5	00101010	Y_3Z_6	00100110	Z_1Y_8	10011100
Z_0Y_8	10011101	Z_2X_8	01011101	Z_3X_8	00111101	Z_4X_7	01110001
Z_5X_7	01101001	Z_6X_7	01100101	Z_1Z_4	10010000	Z_1Z_5	10001000
Z_1Z_6	10000100	Z_0Z_5	10001001	Z_0Z_6	10000101	Z_2Y_4	01010001
Z_2Y_5	01001001	Z_2Y_6	01000101	Z_2Y_8	01011100	Z_3Y_4	00110001
Z_3Y_5	00101001	Z_3Y_6	00100101	Z_3Y_8	00111100	Z_4Y_7	01110011
Z_5Y_7	01101011	Z_6Y_7	01100111	Z_2Z_4	01010000	Z_2Z_5	01001000
Z_2Z_6	01000100	Z_3Z_4	00110000	Z_3Z_5	00101000	Z_3Z_6	00100100
$Z_4Z_7X_8$	00001111	$Z_5Z_7X_8$	00010111	$Z_5Z_6Z_7$	00001110	$Z_4Z_6Z_7$	00010110
$Z_0Y_7Y_8$	11111110	$Z_1Y_7Y_8$	11111111	$Z_5Z_6X_7$	01101101	$Z_4Z_6X_7$	01110101
$Z_4Z_5X_7$	01111001	$Z_5Y_6X_7$	01101100	$Z_4Y_6X_7$	01110100	$Z_4Y_5X_7$	01111000
$Z_0Z_2Y_8$	11011101	$Z_0Z_3Y_8$	10111101	$Z_0Z_4Y_7$	11110010	$Y_0Z_5Z_6$	10001110
$Z_0Z_5Y_7$	11101010	$Y_0Z_4Z_6$	10010110	$Z_0Z_6Y_7$	11100110	$Z_0X_7Y_8$	11111100
$Z_1Z_2Y_8$	11011100	$Z_1Z_3Y_8$	10111100	$Z_1Z_4Y_7$	11110011	$Y_1Z_5Z_6$	10001111
$Z_1Z_5Y_7$	11101011	$Y_1Z_4Z_6$	10010111	$Z_1Z_6Y_7$	11100111	$Z_1X_7Y_8$	11111101
$Y_2Z_5Z_6$	01001110	$Y_2Z_4Z_6$	01010110	$Y_2Z_4Z_5$	01011010	$Y_3Z_5Z_6$	00101110
$Y_3Z_4Z_6$	00110110	$Y_3Z_4Z_5$	00111010	$Z_5Z_6Y_7$	01101111	$Z_4Z_6Y_7$	01110111
$Z_4Z_5Y_7$	01111011	$Z_0Z_2Z_4$	11010001	$Z_0Z_2Z_5$	11001001	$Z_0Z_2Z_6$	11000101
$Z_0Z_3Z_4$	10110001	$Z_0Z_3Z_5$	10101001	$Z_0Z_3Z_6$	10100101	$Z_0Z_4X_7$	11110000
$Z_0Z_5X_7$	11101000	$Z_0Z_6X_7$	11100100	$Z_1Z_2Z_4$	11010000	$Z_1Z_2Z_5$	11001000
$Z_1Z_2Z_6$	11000100	$Z_1Z_3Z_4$	10110000	$Z_1Z_3Z_5$	10101000	$Z_1Z_3Z_6$	10100100
$Z_1Z_4X_7$	11110001	$Z_1Z_5X_7$	11101001	$Z_1Z_6X_7$	11100101	$Y_2Z_5Y_6$	01001111
$Y_2Z_4Y_6$	01010111	$Y_2Z_4Y_5$	01011011	$Y_3Z_5Y_6$	00101111	$Y_3Z_4Y_6$	00110111
$Y_3Z_4Y_5$	00111011	$Z_5Y_6Y_7$	01101110	$Z_4Y_6Y_7$	01110110	$Z_4Y_5Y_7$	01111010
$Z_0Y_2Y_8$	11011111	$Z_0Y_3Y_8$	10111111	$Z_1Y_2Y_8$	11011110	$Z_1Y_3Y_8$	10111110
$Z_0Y_2Z_4$	11010011	$Z_0Y_2Z_5$	11001011	$Z_0Y_2Z_6$	11000111	$Z_0Y_3Z_4$	10110011
$Z_0Y_3Z_5$	10101011	$Z_0Y_3Z_6$	10100111	$Z_1Y_2Z_4$	11010010	$Z_1Y_2Z_5$	11001010
$Z_1Y_2Z_6$	11000110	$Z_1Y_3Z_4$	10110010	$Z_1Y_3Z_5$	10101010	$Z_1Y_3Z_6$	10100110
$Z_0Z_5Z_6$	10001101	$Z_0Z_4Z_6$	10010101	$Z_1Z_5Z_6$	10001100	$Z_1Z_4Z_6$	10010100
$Z_1Z_4Z_5$	10011000	$Z_2Z_5Z_6$	01001100	$Z_2Z_4Z_6$	01010100	$Z_2Z_4Z_5$	01011000
$Z_3Z_5Z_6$	00101100	$Z_3Z_4Z_6$	00110100	$Z_3Z_4Z_5$	00111000	$Z_2Z_5Y_6$	01001101
$Z_2Z_4Y_6$	01010101	$Z_2Z_4Y_5$	01011001	$Z_3Z_5Y_6$	00101101	$Z_3Z_4Y_6$	00110101
$Z_3Z_4Y_5$	00111001	$Z_1Z_5Z_6Y_7$	11101111	$Z_1Z_4Z_6Y_7$	11110111	$Z_1Z_4Z_5Y_7$	11111011
$Z_0Z_5Z_6Y_7$	11101110	$Z_0Z_4Z_6Y_7$	11110110	$Z_0Z_4Z_5Y_7$	11111010	$Z_1Z_2Z_5Z_6$	11001100
$Z_1Z_2Z_4Z_6$	11010100	$Z_1Z_2Z_4Z_5$	11011000	$Z_1Z_3Z_5Z_6$	10101100	$Z_1Z_3Z_4Z_6$	10110100
$Z_1Z_3Z_4Z_5$	10111000	$Z_1Z_5Z_6X_7$	11101101	$Z_1Z_4Z_6X_7$	11110101	$Z_1Z_4Z_5X_7$	11111001
$Z_0Z_2Z_5Z_6$	11001101	$Z_0Z_2Z_4Z_6$	11010101	$Z_0Z_2Z_4Z_5$	11011001	$Z_0Z_3Z_5Z_6$	10101101
$Z_0Z_3Z_4Z_6$	10110101	$Z_0Z_3Z_4Z_5$	10111001	$Z_0Z_5Z_6X_7$	11101100	$Z_0Z_4Z_6X_7$	11110100
$Z_0Z_4Z_5X_7$	11111000	$Z_1Y_2Z_5Z_6$	11001110	$Z_1Y_2Z_4Z_6$	11010110	$Z_1Y_2Z_4Z_5$	11011010
$Z_1Y_3Z_5Z_6$	10101110	$Z_1Y_3Z_4Z_6$	10110110	$Z_1Y_3Z_4Z_5$	10111010	$Z_0Y_2Z_5Z_6$	11001111
$Z_0Y_2Z_4Z_6$	11010111	$Z_0Y_2Z_4Z_5$	11011011	$Z_0Y_3Z_5Z_6$	10101111	$Z_0Y_3Z_4Z_6$	10110111

5. $[[10, 1, 3]]$ code

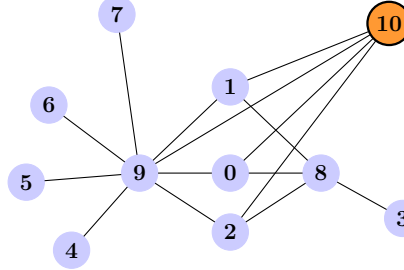


FIG. S5. Ten qubit graph state(blue) with one message qubit(orange).

Stabilizer generating set:

$$\langle X_0X_1, X_0X_2, X_3Z_8, X_4Z_9, X_5Z_9, X_6Z_9, X_7Z_9, Z_0Z_1Z_2Z_3X_8, Y_0Z_1Z_2Z_4Z_5Z_6Z_7Z_8Y_9 \rangle$$

Logical operators:

$$X_l = X_0Z_8Z_9, \quad Z_l = Z_0Z_1Z_2Z_9.$$

Error (Z)	Syndrome (Z)	Error (X)	Syndrome (X)	Error (Y)	Syndrome (Y)
Z_0	110000001	X_0	000000011	Y_0	110000010
Z_1	100000000	X_1	000000011	Y_1	100000011
Z_2	010000000	X_2	000000011	Y_2	010000011
Z_3	001000000	X_3	000000010	Y_3	001000010
Z_4	000100000	X_4	000000001	Y_4	000100001
Z_5	000010000	X_5	000000001	Y_5	000010001
Z_6	000001000	X_6	000000001	Y_6	000001001
Z_7	000000100	X_7	000000001	Y_7	000000101
Z_8	000000010	X_8	001000001	Y_8	001000011
Z_9	000000001	X_9	000111101	Y_9	000111100

TABLE XIII. Single-qubit error syndromes for the $[[10, 1, 3]]$ code

$Z_0Z_1Z_2Z_3X_8 \rightarrow Z_0Z_3Z_1X_8Z_2$		$Y_0Z_1Z_2Z_4Z_5Z_6Z_7Z_8Y_9 \rightarrow Z_4Y_0Z_5Z_1Z_6Z_2Z_7Z_8Y_9$	
Error	Syndrome	Error	Syndrome
$Z_0Z_3Y_1$	011000010	Z_4X_0	000100011
Z_2X_8	011000001	Z_4Y_0	110100010
Z_2Z_8	010000010	Z_4Z_0	110100001
Z_2Y_8	011000011	$Z_4Y_0X_5$	110100011
$Z_0Z_3X_1$	111000010	$Z_4Y_0Y_5$	110110011
Z_0X_3	110000011	$Z_4Y_0Z_5$	110110010
Z_0Y_3	111000011	$Z_4Y_0Z_5X_1$	110110001
Z_0Z_3	111000001	$Z_4Y_0Z_5Y_1$	010110001
–	–	$Z_4Y_0Z_5Z_1$	010110010
–	–	$Z_4Y_0Z_5Z_1X_6$	010110011
–	–	$Z_4Y_0Z_5Z_1Y_6$	010111011
–	–	$Z_2Z_7Z_8Y_9$	010111010
–	–	$Y_2Z_7Z_8Y_9$	010111001
–	–	$X_2Z_7Z_8Y_9$	000111001
–	–	$Z_7Z_8Y_9$	000111010
–	–	$Y_7Z_8Y_9$	000111011
–	–	$X_7Z_8Y_9$	000111111
–	–	Z_8Y_9	000111110
–	–	Y_8Y_9	001111111
–	–	X_8Y_9	001111101

TABLE XIV. Propagated errors in the $[[10, 1, 3]]$ code with their syndromes under reordering stabilizers.TABLE XV: Left-alone syndromes used in the lookup table for the $[[10, 1, 3]]$ code.

Error	Syndrome	Error	Syndrome	Error	Syndrome	Error	Syndrome
$Z_2Z_6Z_7Y_8$	011001111	Z_3Y_9	001111100	Z_4Z_8	000100010	Z_5Z_8	000010010
Z_6Z_8	000001010	Z_7Z_8	000000110	Y_5Z_8	000010011	Y_6Z_8	000001011
Y_7Z_8	000000111	Z_1Z_2	110000000	Y_0X_9	110111111	Z_1Z_9	100000001
Z_1Z_8	100000010	Z_1Y_3	101000010	Y_1X_9	100111110	Z_2Z_9	010000001
Y_2X_9	010111110	Z_3Z_4	001100000	Z_4Y_9	000011100	Z_3Z_5	001010000
Z_5Y_9	000101100	Z_3Z_6	001001000	Z_6Y_9	000110100	Z_3Z_7	001000100
Z_7Y_9	000111000	Y_3Y_9	001111110	Z_0X_8	111000000	Y_0Y_5	110010011
Y_0Y_6	110001011	Y_0Y_7	110000111	Y_0Y_9	110111110	Z_1X_8	101000001
Y_1Y_4	100100010	Y_1Y_5	100010010	Y_1Y_6	100001010	Y_1Y_7	100000110
Z_1Z_3	101000000	Y_1Y_9	100111111	Y_2Y_4	010100010	Y_2Y_5	010010010
Y_2Y_6	010001010	Y_2Y_7	010000110	Z_2Z_3	011000000	Y_2Y_9	010111111
Z_4Y_8	001100011	Z_5Y_8	001010011	Z_6Y_8	001001011	Z_7Y_8	001000111
Z_4Z_5	000110000	Z_4Z_6	000101000	Z_4Z_7	000100100	Y_3Z_4	001100010
Z_4X_9	000011101	Z_5Z_6	000011000	Z_5Z_7	000010100	Y_3Z_5	001010010
Z_5X_9	000101101	Z_6Z_7	000001100	Y_3Z_6	001001010	Z_6X_9	000110101
Y_3Z_7	001000110	Y_0Z_5	110010010	Y_0Z_6	110001010	Y_0Z_7	110000110
Z_1Y_8	101000011	Y_1Z_4	100100011	Y_1Z_5	100010011	Y_1Z_6	100001011
Y_1Z_7	100000111	Y_2Z_4	010100011	Y_2Z_5	010010011	Y_2Z_6	010001011
Y_2Z_7	010000111	Z_4Y_5	000110001	Z_4Y_6	000101001	Z_4Y_7	000100101
Z_5Y_6	000011001	Z_5Y_7	000010101	Z_6Y_7	000001101	Z_0X_9	110111100
Z_1X_9	100111101	Z_2X_9	010111101	Z_3Y_4	001100001	Z_3Z_5	001010001
Z_3Y_6	001001001	Z_3Y_7	001000101	Z_0Y_4	110100000	Z_0Y_5	110010000
Z_0Y_6	110001000	Z_0Y_7	110000100	Z_0Y_9	110111101	Z_1Y_4	100100001
Z_1Y_5	100010001	Z_1Y_6	100001001	Z_1Y_7	100000101	Z_1Y_9	100111100
Z_2Y_4	010100001	Z_2Y_5	010010001	Z_2Y_6	010001001	Z_2Y_7	010000101
Z_2Y_9	010111100	Z_0Z_5	110010001	Z_0Z_6	110001001	Z_0Z_7	110000101
Z_1Z_4	100100000	Z_1Z_5	100010000	Z_1Z_6	100001000	Z_1Z_7	100000100
Z_2Z_4	010100000	Z_2Z_5	010010000	Z_2Z_6	010001000	Z_2Z_7	010000100
$Z_4Z_8X_9$	000011111	$Z_5Z_8X_9$	000101111	$Z_6Z_8X_9$	000110111	$Z_4Z_8Y_9$	000011110
$Z_5Z_8Y_9$	000101110	$Z_6Z_8Y_9$	000110110	$Z_4Y_5Z_8$	000110011	$Z_4Y_6Z_8$	000101011

Error	Syndrome	Error	Syndrome	Error	Syndrome	Error	Syndrome
$Z_4Y_7Z_8$	000100111	$Z_5Y_6Z_8$	000011011	$Z_5Y_7Z_8$	000010111	$Z_6Y_7Z_8$	000001111
$Z_4Z_5Z_8$	000110010	$Z_4Z_6Z_8$	000101010	$Z_4Z_7Z_8$	000100110	$Z_5Z_6Z_8$	000011010
$Z_5Z_7Z_8$	000010110	$Z_6Z_7Z_8$	000001110	$Z_0Y_8Y_9$	111111110	$Z_1Y_8Y_9$	101111111
$Z_2Y_8Y_9$	011111111	$Z_3Z_4X_9$	001011101	$Z_3Z_5X_9$	001101101	$Z_3Z_6X_9$	001110101
$Z_3Z_7X_9$	001111001	$Z_0Y_3Y_9$	111111111	$Z_1Y_3Y_9$	101111110	$Z_2Y_3Y_9$	011111110
$Z_3Z_4Y_9$	001011100	$Z_3Z_5Y_9$	001101100	$Z_3Z_6Y_9$	001110100	$Z_3Z_7Y_9$	001111000
$Z_0Z_3Y_9$	111111101	$Z_0Z_4Y_8$	111100010	$Y_0Z_4Y_9$	110011110	$Z_0Z_5Y_8$	111010010
$Y_0Z_5Y_9$	110101110	$Z_0Z_6Y_8$	111001010	$Y_0Z_6Y_9$	110110110	$Z_0Z_7Y_8$	111000110
$Y_0Z_7Y_9$	110111010	$Z_0Z_3X_9$	111111100	$Z_1Z_3Y_9$	101111100	$Z_1Z_4Y_8$	101100011
$Y_1Z_4Y_9$	100011111	$Z_1Z_5Y_8$	101010011	$Y_1Z_5Y_9$	100101111	$Z_1Z_6Y_8$	101001011
$Y_1Z_6Y_9$	100110111	$Z_1Z_7Y_8$	101000111	$Y_1Z_7Y_9$	100111011	$Z_1Z_3X_9$	101111101
$Z_2Z_3Y_9$	011111100	$Z_2Z_4Y_8$	011100011	$Y_2Z_4Y_9$	010011111	$Z_2Z_5Y_8$	011010011
$Y_2Z_5Y_9$	010101111	$Z_2Z_6Y_8$	011001011	$Y_2Z_6Y_9$	010110111	$Z_2Z_7Y_8$	011000111
$Z_2Z_3X_9$	011111101	$Z_4Y_8X_9$	001011110	$Z_5Y_8X_9$	001101110	$Z_6Y_8X_9$	001110110
$Z_7Y_8X_9$	001111010	$Z_3Z_4Y_5$	001110001	$Z_3Z_4Y_6$	001101001	$Z_3Z_4Y_7$	001100101
$Z_4Y_8Y_9$	001011111	$Z_3Z_5Y_6$	001011001	$Z_3Z_5Y_7$	001010101	$Z_5Y_8Y_9$	001101111
$Z_3Z_6Y_7$	001001101	$Z_6Y_8Y_9$	001110111	$Z_7Y_8Y_9$	001111011	$Z_0Z_3Z_4$	111100001
$Z_0Z_3Z_5$	111010001	$Z_0Z_3Z_6$	111001001	$Z_0Z_3Z_7$	111000101	$Y_0Z_4Z_6$	110101010
$Y_0Z_4Z_7$	110100110	$Z_0Z_3Y_4$	111100000	$Y_0Z_4X_9$	110011111	$Y_0Z_5Z_6$	110011010
$Y_0Z_5Z_7$	110010110	$Z_0Z_3Y_5$	111010000	$Y_0Z_5X_9$	110101111	$Y_0Z_6Z_7$	110001110
$Z_0Z_3Y_6$	111001000	$Y_0Z_6X_9$	110110111	$Z_0Z_3Y_7$	111000100	$Y_0Z_7X_9$	110111011
$Z_1Z_3Z_4$	101100000	$Z_1Z_3Z_5$	101010000	$Z_1Z_3Z_6$	101001000	$Z_1Z_3Z_7$	101000100
$Y_1Z_4Z_5$	100110011	$Y_1Z_4Z_6$	100101011	$Y_1Z_4Z_7$	100100111	$Z_1Z_3Y_4$	101100001
$Y_1Z_4X_9$	100011110	$Y_1Z_5Z_6$	100011011	$Y_1Z_5Z_7$	100010111	$Z_1Z_3Y_5$	101010001
$Y_1Z_5X_9$	100101110	$Y_1Z_6Z_7$	100001111	$Z_1Z_3Y_6$	101001001	$Y_1Z_6X_9$	100110110
$Z_1Z_3Y_7$	101000101	$Y_1Z_7X_9$	100111010	$Z_2Z_3Z_4$	011100000	$Z_2Z_3Z_5$	011010000
$Z_2Z_3Z_6$	011001000	$Z_2Z_3Z_7$	011000100	$Y_2Z_4Z_6$	010101011	$Y_2Z_4Z_7$	010100111
$Z_2Z_3Y_4$	011100001	$Y_2Z_4X_9$	010011110	$Y_2Z_5Z_6$	010011011	$Y_2Z_5Z_7$	010010111
$Z_2Z_3Y_5$	011010001	$Y_2Z_5X_9$	010101110	$Y_2Z_6Z_7$	010001111	$Z_2Z_3Y_6$	011001001
$Y_2Z_6X_9$	010110110	$Z_2Z_3Y_7$	011000101	$Z_4Y_5Y_8$	001110010	$Z_4Y_6Y_8$	001101010
$Z_4Y_7Y_8$	001100110	$Z_5Y_6Y_8$	001011010	$Z_5Y_7Y_8$	001010110	$Z_6Y_7Y_8$	001001110
$Z_4Z_5Y_8$	001110011	$Z_4Z_6Y_8$	001101011	$Z_4Z_7Y_8$	001100111	$Z_5Z_6Y_8$	001011011
$Z_5Z_7Y_8$	001010111	$Z_6Z_7Y_8$	001001111	$Y_0Z_4Y_6$	110101011	$Y_0Z_4Y_7$	110100111
$Y_0Z_5Y_6$	110011011	$Y_0Z_5Y_7$	110010111	$Y_0Z_6Y_7$	110001111	$Y_1Z_4Y_5$	100110010
$Y_1Z_4Y_6$	100101010	$Y_1Z_4Y_7$	100100110	$Y_1Z_5Y_6$	100011010	$Y_1Z_5Y_7$	100010110
$Y_1Z_6Y_7$	100001110	$Y_2Z_4Y_6$	010101010	$Y_2Z_4Y_7$	010100110	$Y_2Z_5Y_6$	010011010
$Y_2Z_5Y_7$	010010110	$Y_2Z_6Y_7$	010001110	$Z_0Y_3Z_4$	111100011	$Z_0Y_3Z_5$	111010011
$Z_0Y_3Z_6$	111001011	$Z_0Y_3Z_7$	111000111	$Z_1Y_3Z_4$	101100010	$Z_1Y_3Z_5$	101010010
$Z_1Y_3Z_6$	101001010	$Z_1Y_3Z_7$	101000110	$Z_2Y_3Z_4$	011100010	$Z_2Y_3Z_5$	011010010
$Z_2Y_3Z_6$	011001010	$Z_2Y_3Z_7$	011000110	$Z_3Z_4Z_5$	001110000	$Z_3Z_4Z_6$	001101000
$Z_3Z_4Z_7$	001100100	$Z_3Z_5Z_6$	001011000	$Z_3Z_5Z_7$	001010100	$Z_3Z_6Z_7$	001001100
$Z_0Z_4Y_9$	110011101	$Z_0Z_5Y_9$	110101101	$Z_0Z_6Y_9$	110110101	$Z_0Z_7Y_9$	110111001
$Z_1Z_4Y_9$	100011100	$Z_1Z_5Y_9$	100101100	$Z_1Z_6Y_9$	100110100	$Z_1Z_7Y_9$	100111000
$Z_2Z_4Y_9$	010011100	$Z_2Z_5Y_9$	010101100	$Z_2Z_6Y_9$	010110100	$Z_2Z_7Y_9$	010111000
$Z_0Z_4Z_6$	110101001	$Z_0Z_4Z_7$	110100101	$Z_0Z_4X_9$	110011100	$Z_0Z_5Z_6$	110011001
$Z_0Z_5Z_7$	110010101	$Z_0Z_5X_9$	110101100	$Z_0Z_6Z_7$	110001101	$Z_0Z_6X_9$	110110100
$Z_0Z_7X_9$	110111100	$Z_1Z_4Z_5$	100110000	$Z_1Z_4Z_6$	100101000	$Z_1Z_4Z_7$	100100100
$Z_1Z_4X_9$	100011101	$Z_1Z_5Z_6$	100011000	$Z_1Z_5Z_7$	100010100	$Z_1Z_5X_9$	100101101
$Z_1Z_6Z_7$	100001110	$Z_1Z_6X_9$	100110101	$Z_1Z_7X_9$	100111001	$Z_2Z_4Z_5$	010110000
$Z_2Z_4Z_6$	010101000	$Z_2Z_4Z_7$	010100100	$Z_2Z_4X_9$	010011101	$Z_2Z_5Z_6$	010011000
$Z_2Z_5Z_7$	010010100	$Z_2Z_5X_9$	010101101	$Z_2Z_6Z_7$	010001100	$Z_2Z_6X_9$	010110101
$Z_0Z_4Y_5$	110111000	$Z_0Z_4Y_6$	110101000	$Z_0Z_4Y_7$	110100100	$Z_0Z_5Y_6$	110011000
$Z_0Z_5Y_7$	110010100	$Z_0Z_6Y_7$	110001100	$Z_1Z_4Y_5$	100110001	$Z_1Z_4Y_6$	100101001
$Z_1Z_4Y_7$	100100101	$Z_1Z_5Y_6$	100011001	$Z_1Z_5Y_7$	100010101	$Z_1Z_6Y_7$	100001101
$Z_2Z_4Y_6$	010101001	$Z_2Z_4Y_7$	010100101	$Z_2Z_5Y_6$	010011001	$Z_2Z_5Y_7$	010010101
$Z_2Z_6Y_7$	010001101	$Z_0Z_4Y_8X_9$	111011111	$Z_0Z_5Y_8X_9$	111101111	$Z_0Z_6Y_8X_9$	111110111
$Z_0Z_7Y_8X_9$	111111011	$Z_1Z_4Y_8X_9$	101011110	$Z_1Z_5Y_8X_9$	101101110	$Z_1Z_6Y_8X_9$	101110110
$Z_1Z_7Y_8X_9$	101111010	$Z_2Z_4Y_8X_9$	011011110	$Z_2Z_5Y_8X_9$	011101110	$Z_2Z_6Y_8X_9$	011110110
$Z_2Z_7Y_8X_9$	011111010	$Z_0Z_4Y_8Y_9$	111011110	$Z_0Z_5Y_8Y_9$	111101110	$Z_0Z_6Y_8Y_9$	111110110
$Z_0Z_7Y_8Y_9$	111111010	$Z_1Z_4Y_8Y_9$	101011111	$Z_1Z_5Y_8Y_9$	101101111	$Z_1Z_6Y_8Y_9$	101110111
$Z_1Z_7Y_8Y_9$	101111011	$Z_2Z_4Y_8Y_9$	011011111	$Z_2Z_5Y_8Y_9$	011101111	$Z_2Z_6Y_8Y_9$	011110111
$Z_2Z_7Y_8Y_9$	011111011	$Z_0Z_3Z_4X_9$	111011100	$Z_0Z_3Z_5X_9$	111101100	$Z_0Z_3Z_6X_9$	111110100

Error	Syndrome	Error	Syndrome	Error	Syndrome	Error	Syndrome
$Z_0 Z_3 Z_7 X_9$	111111000	$Z_0 Z_4 Y_5 Y_8$	111110011	$Z_0 Z_4 Y_6 Y_8$	111101011	$Z_0 Z_4 Y_7 Y_8$	111100111
$Z_0 Z_3 Z_4 Y_9$	111011101	$Z_0 Z_5 Y_6 Y_8$	111011011	$Z_0 Z_5 Y_7 Y_8$	111010111	$Z_0 Z_3 Z_5 Y_9$	111101101
$Z_0 Z_6 Y_7 Y_8$	111001111	$Z_0 Z_3 Z_6 Y_9$	111110101	$Z_0 Z_3 Z_7 Y_9$	111111001	$Z_1 Z_3 Z_4 X_9$	101011101
$Z_1 Z_3 Z_5 X_9$	101101101	$Z_1 Z_3 Z_6 X_9$	101110101	$Z_1 Z_3 Z_7 X_9$	101111001	$Z_1 Z_4 Y_5 Y_8$	101110010
$Z_1 Z_4 Y_6 Y_8$	101101010	$Z_1 Z_4 Y_7 Y_8$	101100110	$Z_1 Z_3 Z_4 Y_9$	101011100	$Z_1 Z_5 Y_6 Y_8$	101011010
$Z_1 Z_5 Y_7 Y_8$	101010110	$Z_1 Z_3 Z_5 Y_9$	101101100	$Z_1 Z_6 Y_7 Y_8$	101001110	$Z_1 Z_3 Z_6 Y_9$	101110100
$Z_1 Z_3 Z_7 Y_9$	101111000	$Z_2 Z_3 Z_4 X_9$	011011101	$Z_2 Z_3 Z_5 X_9$	011101101	$Z_2 Z_3 Z_6 X_9$	011110101
$Z_2 Z_3 Z_7 X_9$	011111001	$Z_2 Z_4 Y_5 Y_8$	011110010	$Z_2 Z_4 Y_6 Y_8$	011101010	$Z_2 Z_4 Y_7 Y_8$	011100110
$Z_2 Z_3 Z_4 Y_9$	011011100	$Z_2 Z_5 Y_6 Y_8$	011011010	$Z_2 Z_5 Y_7 Y_8$	011010110	$Z_2 Z_3 Z_5 Y_9$	011101100
$Z_2 Z_6 Y_7 Y_8$	011001110	$Z_2 Z_3 Z_6 Y_9$	011110100	$Z_2 Z_3 Z_7 Y_9$	011111000	$Z_0 Z_3 Z_4 Y_5$	111110000
$Z_0 Z_3 Z_4 Y_6$	111101000	$Z_0 Z_3 Z_4 Y_7$	111100100	$Z_0 Z_3 Z_5 Y_6$	111011000	$Z_0 Z_3 Z_5 Y_7$	111010100
$Z_0 Z_3 Z_6 Y_7$	111001100	$Z_0 Z_3 Z_4 Z_5$	111110001	$Z_0 Z_3 Z_4 Z_6$	111101001	$Z_0 Z_3 Z_4 Z_7$	111100101
$Z_0 Z_3 Z_5 Z_6$	111011001	$Z_0 Z_3 Z_5 Z_7$	111010101	$Z_0 Z_3 Z_6 Z_7$	111001101	$Z_1 Z_3 Z_4 Y_5$	101110001
$Z_1 Z_3 Z_4 Y_6$	101101001	$Z_1 Z_3 Z_4 Y_7$	101100101	$Z_1 Z_3 Z_5 Y_6$	101011001	$Z_1 Z_3 Z_5 Y_7$	101010101
$Z_1 Z_3 Z_6 Y_7$	101001101	$Z_1 Z_3 Z_4 Z_5$	101110000	$Z_1 Z_3 Z_4 Z_6$	101101000	$Z_1 Z_3 Z_4 Z_7$	101100100
$Z_1 Z_3 Z_5 Z_6$	101011000	$Z_1 Z_3 Z_5 Z_7$	101010100	$Z_1 Z_3 Z_6 Z_7$	101001100	$Z_2 Z_3 Z_4 Y_5$	011110001
$Z_2 Z_3 Z_4 Y_6$	011101001	$Z_2 Z_3 Z_4 Y_7$	011100101	$Z_2 Z_3 Z_5 Y_6$	011011001	$Z_2 Z_3 Z_5 Y_7$	011010101
$Z_2 Z_3 Z_6 Y_7$	011001101	$Z_2 Z_3 Z_4 Z_5$	011110000	$Z_2 Z_3 Z_4 Z_6$	011101000	$Z_2 Z_3 Z_4 Z_7$	011100100
$Z_2 Z_3 Z_5 Z_6$	011011000	$Z_2 Z_3 Z_5 Z_7$	011010100	$Z_2 Z_3 Z_6 Z_7$	011001100	$Z_0 Z_4 Z_5 Y_8$	111110010
$Z_0 Z_4 Z_6 Y_8$	111101010	$Z_0 Z_4 Z_7 Y_8$	111100110	$Z_0 Z_5 Z_6 Y_8$	111011010	$Z_0 Z_5 Z_7 Y_8$	111010110
$Z_0 Z_6 Z_7 Y_8$	111001110	$Z_1 Z_4 Z_5 Y_8$	101110011	$Z_1 Z_4 Z_6 Y_8$	101101011	$Z_1 Z_4 Z_7 Y_8$	101100111
$Z_1 Z_5 Z_6 Y_8$	101011011	$Z_1 Z_5 Z_7 Y_8$	101010111	$Z_1 Z_6 Z_7 Y_8$	101001111	$Z_2 Z_4 Z_5 Y_8$	011110011
$Z_2 Z_4 Z_6 Y_8$	011101011	$Z_2 Z_4 Z_7 Y_8$	011100111	$Z_2 Z_5 Z_6 Y_8$	011011011	$Z_2 Z_5 Z_7 Y_8$	011010111